

N

Natural Atomic Orbital (NAO)

A valence shell atomic orbital whose derivation involves diagonalizing the localized block of the electron density matrix with atomic basis functions $\chi_i(A)$. See *Population Analyses for Semiempirical Methods*.

Natural Bond Orbital (NBO)

A symmetrically orthogonalized directed hybrid orbital derived through unitary transformation of natural atomic orbitals centered on a particular atom. See *Population Analyses for Semiempirical Methods*.

Natural Bond Orbital Methods

Frank Weinhold

University of Wisconsin, Madison, WI, USA

1	Introduction	1792
2	Background of Natural Population Analysis Methods	1793
3	Natural Localized Orbitals	1794
4	Natural Localized Configurations	1801
5	Localized NAO/NBO Analysis of Energy and Other Molecular Properties	1805
6	Other NAO/NBO 'Enhanced' Bonding Indices and Hückel-like Quantities	1808
7	Summary and Outlook	1809
8	Related Articles	1810
9	References	1810

Abbreviations

BONDO = bond orbital - neglect of differential overlap (SCF-MO); GIAO = gauge-including atomic orbital; L = Lewis-type (or localized); LC-BO = linear combination of bond orbitals; LCNBO = linear combination of NBOs; LMO = localized molecular orbital; MSPNBO = maximum spin-paired NBO; NBBP = natural bond-bond polarizability; NBO = natural bond orbital; NCS = natural chemical shielding; NEDA = natural energy decomposition analysis; NHO = natural hybrid orbital; NL = non-Lewis-type (or

non-localized); NLMO = natural localized molecular orbital; NMB = natural minimal basis; NRB = natural Rydberg basis (orthogonal complement of NMB); NRT = natural resonance theory; OWSO = occupancy-weighted symmetric orthogonalization; PNAO = pre-orthogonal NAO; PNBO = pre-orthogonal NBO; PNHO = pre-orthogonal NHO; PNLMO = pre-orthogonal NLMO; TB = through-bond; TS = through-space.

1 INTRODUCTION

The term 'natural bond orbital methods' encompasses a suite of methods, including natural population analysis (NPA), for describing the N -electron wavefunction $\psi(1, 2, \dots, N)$ in terms of localized orbitals or configurations that are closely tied to chemical bonding concepts.¹ Underlying such methods are the sets of intrinsic 'natural' atomic orbitals (NAOs), hybrid orbitals (NHOs), and bond orbitals (NBOs), as well as associated semi-localized molecular orbitals (NLMOs), which are in close correspondence with the chemist's *Lewis structure* representation. Each such localized basis set is complete and orthonormal, optimally chosen with respect to the molecular environment to describe the *electron density* and other properties in the most rapidly convergent fashion. The populations (occupancies) of these orbitals are therefore highly condensed in the few most important members (i.e., those corresponding to the formal *minimal basis* in the NAO case or to the Lewis-like bonds and lone pairs in the NBO case), allowing the remaining contributions to be satisfactorily treated as small corrections by standard perturbative techniques. As a general characteristic, the NAO/NBO-based methods make no special reference to the form of wavefunction or density and may therefore be used to compare results from arbitrary levels of semi-empirical, *ab initio*, or density functional theory, including (in principle) the exact solution of *Schrödinger's equation*.

The associated natural resonance theory (NRT) provides a related population weighting for localized N -e *configurational* functions, corresponding to the chemist's 'resonance structure' picture. Each resonance structure depicts a pattern of bonds and lone pairs (described by corresponding optimal NBOs) whose relative weighting in the delocalized *resonance hybrid* can be determined by the NRT variational principle (as described below). Such resonance weights are useful in approximating a molecular property as the weighted average of corresponding properties for the idealized localized resonance structures, with non-negative weights summing to unity. From these weightings one can also determine the natural bond order P_{AB} as the weighted average of the number of A-B bonds in each contributing resonance structure. The NRT quantities thus form a quantitative bridge to many qualitative resonance structure concepts.

NBOs also underlie novel methods for describing *electron correlation* in localized terms. A starting NBO configuration can be used to construct localized multi-configurational CAS/NBO wavefunctions with transferable correlation contributions corresponding to the familiar 'types' (left-right, in-out, angular) in diatomic molecules.

Associated with the localized NAO/NBO orbitals and population measures are allied techniques for analyzing molecular

properties, such as intramolecular and intermolecular interaction energies, dipole moments, steric repulsions, and NMR chemical shielding tensor components. In addition, NAO/NBO techniques can be used to improve the calculation of older bonding indices (such as the Wiberg bond index or bond-bond polarizability) and to show the connection between earlier Hückel-like and modern *ab initio* wavefunctions. Brief surveys of both types of applications will be presented below. NBO applications to specific chemical problems^{1,2} are beyond the scope of this article.

The NAO/NBO/NRT algorithms and associated analyses are implemented in a computer program (currently, NBO 4.0) which is integrated into a variety of modern electronic structure packages and presents a uniform interface (user options, output format, etc.) for users of many program systems. Thus, it is useful to include reference to standard program keywords that initiate the method under description. Reference should be made to the NBO program manual and source code (as well as the original papers) for additional implementation details, options, numerical thresholds, etc., beyond the scope of this article. Throughout this article, the formaldehyde molecule will be used as a simple example to illustrate NAO/NBO/NRT concepts.

2 BACKGROUND OF NATURAL POPULATION ANALYSIS METHODS

Logically, the NPA methods may be considered to build upon three previous lines of quantum chemistry development:

- (i) *Mulliken population analysis*. Within the framework of LCAO-MO theory, Mulliken³ introduced a procedure to assign occupancies to each member of the (generally non-orthogonal) atomic orbital (AO) basis set, thereby determining the 'Mulliken charges' on each atom. Historically, *Mulliken analysis* has been the most widely used methodology to interpret wavefunctions in chemical terms. However, this procedure often exhibits severe physical and mathematical pathologies, such as instabilities with respect to basis extensions (e.g., *diffuse functions*), unphysical negative or Pauli-violating populations, and conspicuous underestimates of ionic character in molecules with large electronegativity differences. These anomalies are essentially eliminated by the NPA procedure, which in addition can be performed on wavefunctions of more general form.
- (ii) *Natural orbitals*. This term refers to the intrinsic orbitals $\{\theta_k\}$ that arise as eigenfunctions of the first-order reduced density operator \hat{F} ,

$$\hat{F}\theta_k = q_k\theta_k \quad (1)$$

which is formed by 'reducing' the wavefunction probability distribution to the single-particle level,

$$\hat{F} = N \int \psi(1, 2, \dots, N) \psi^*(1', 2, \dots, N) d\tau_2 \dots d\tau_N \quad (2)$$

and whose eigenorbitals are hence 'natural' to ψ itself. As shown by Löwdin⁴ and others, rigorous quantum-mechanical questions involving subsystems of an N -particle system are best formulated in terms of reduced density operators. In particular, the squared probability amplitude $|\langle\psi(1, 2, \dots, N)|\phi(1)\rangle|^2$ that an electron of $\psi(1, 2, \dots, N)$ is 'in' orbital ϕ

(i.e., the population of $\phi(1)$ in the wavefunction) is rigorously expressed, for any possible orbital ϕ , as

$$q_\phi = \langle\phi|\hat{F}|\phi\rangle \quad (3)$$

The occupancies q_ϕ are intrinsically non-negative and limited by the *Pauli exclusion principle*, e.g., for spatial orbital $\phi(\mathbf{r})$,

$$0 \leq q_\phi \leq 2 \quad (4a)$$

(The analogous restriction $q_\phi \leq 1$ applies to *spin orbitals*, but for simplicity we restrict discussion to the closed-shell case.) Moreover, the sum of occupancies q_k over any complete orthonormal set $\{\phi_k\}$ accounts for all N electrons,

$$\sum_k \langle\phi_k|\hat{F}|\phi_k\rangle = \sum_k q_k = \text{Tr}(\hat{F}) = N \quad (4b)$$

As remarked above, Mulliken populations ('gross' or 'net') commonly fail to satisfy the physical constraints (4a, b). The natural orbitals (NOs) $\{\theta_k\}$ of equation (1) are intrinsically best possible for condensing maximum occupancy in the smallest possible number of orbitals. However, they are rather unsuitable for chemical analysis, since they transform as irreducible representations of the full symmetry group of \hat{F} (the symmetry of the Hamiltonian) and thus appear delocalized over all nuclear centers and highly non-transferable. In this respect, NOs are similar to *canonical molecular orbitals* (to which they reduce in the uncorrelated Hartree-Fock limit). In contrast, the NBOs retain the high occupancy of NOs, but have local one- and two-center character that takes advantage of the high transferability of localized electron pairs of the molecular Lewis structure.

(iii) *Equivalent Localized Orbitals*. As shown by Lennard-Jones and Pople,⁵ based on a theorem of Fock,⁶ the canonical MOs may be unitarily transformed to equivalent *localized molecular orbitals* (LMOs). Such transformations leave the *Hartree-Fock* wavefunction, energy, and other properties invariant, so that LMOs are equally 'true' molecular orbitals (with exact double-occupancy) for any chosen localizing criterion. Minimization of electron repulsions (Edmiston-Ruedenberg⁷) or maximization of mean-squared orbital centroid separation (Boys⁸) leads to LMOs of lower symmetry and increased bond-like character. However, these LMOs are still found to manifest 'delocalization tails' that limit the transferability to other molecules, and no criterion of energy, density, or other measurable property distinguishes whether one set of LMOs is better than any other. In contrast, the NBO populations provide a precise measure of how the orbital form can be optimized to maximally describe the electron density, and these orbitals achieve significantly higher transferability than LMOs.⁹

Historically, NPA methods evolved along a more circuitous route. Brunck and Weinhold¹⁰ originally developed a bond-orbital formulation of SCF-MO theory to analyze patterns of through-bond coupling in the framework of semi-empirical CNDO/INDO methods. Each 'nominal' bond orbital b_{AB} was of the standard form $b_{AB} = c_A h_A + c_B h_B$, composed of idealized sp^n Pauling-type hybrids h_A , h_B and Coulson-type polarization coefficients c_A , c_B (determined from relative atomic electronegativities). However, it was recognized that the LCBO-MO expansion must also incorporate the complementary antibond functions $b_{AB}^* = c_B h_A - c_A h_B$, and that

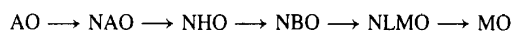
the relative weightings (occupancies) of the latter orbitals are sensitively dependent on the chosen hybrids and polarization coefficients. One can therefore define a mathematically optimal set of 'natural' hybrids¹¹ and polarization coefficients that minimize the b_{AB}^* contributions (or equivalently, maximize the b_{AB} contributions) to occupied MOs. Such maximum-occupancy b_{AB} orbitals were first introduced as 'natural bond orbitals' by Foster and Weinhold¹² and implemented in the BONDO program¹³ (essentially the same algorithm presented in Section 3.2.1 below) for general CNDO/INDO wavefunctions. A fundamental obstacle to extending this formalism to *ab initio* levels was presented by the fact that the common *ab initio* basis AOs are neither orthogonal nor remotely optimal to serve as the 'effective valence shell AOs' assumed in CNDO/INDO theory. Initial attempts to use Löwdin-orthogonalized AOs for this purpose proved futile.¹⁴ Thus, the breakthrough to *ab initio* NBO theory¹⁵ was discovery of the improved 'natural' atomic orbitals (NAOs)¹⁶ that extend the maximum occupancy concept back to the AO level. The NAOs solve many problems of traditional Mulliken population analysis, while allowing a relatively straightforward extension of NBO algorithms from the CNDO/INDO framework (where AOs and NAOs are identical) to general *ab initio* levels of SCF and post-SCF theory, as described below.

Philosophically and mathematically, the NPA methods are wavefunction-oriented, based on variational and perturbation-theoretic use of Hilbert space partitioning to define 'model chemistry' constructs. For a system described by Schrödinger's equation, $\hat{H}\psi = E\psi$, it is advantageous to formulate a physical model in terms of a well-defined 'model Hamiltonian' $\hat{H}^{(0)}$, such that standard *perturbation theory* can be used to assess the corrections to the model, to determine which of several alternative model $\hat{H}^{(0)}$'s is uniquely best (gives most rapid perturbative convergence to the true solution), and so forth. Moreover, such a model $\hat{H}^{(0)}$ can be directly formulated in terms of a projection operator¹⁷ \hat{P} that specifies a particular Hilbert space partitioning (with orthogonal complement \hat{Q} satisfying $\hat{P} + \hat{Q} = 1$) such that $\hat{H}^{(0)} = \hat{P}\hat{H}\hat{P}$, 'the \hat{P} -block of the matrix representation of \hat{H} .' For example, if \hat{P} spans the set of NAOs of atom A, and \hat{Q} those of B, in a system with Hamiltonian $\hat{H} = \hat{H}_A + \hat{H}_B + \hat{H}_{AB}$, then as $R_{AB} \rightarrow \infty$ the projected $\hat{H}^{(0)} = \hat{P}\hat{H}\hat{P}$ becomes identical to \hat{H}_A (or more precisely, its variational matrix representation in the chosen basis set) and the NAOs become the atomic natural orbitals of isolated atom A. However, $\hat{H}^{(0)}$ continues to serve as a model of 'atom A in the A-B molecule' for all finite R_{AB} , with the NAOs as its natural orbitals. The projective technique generally allows different model types to be ranked and the optimal model of a given type to be determined; for example, if \hat{P} projects onto a single-determinantal wavefunction in a specified orbital subspace, the best such $\hat{H}^{(0)}$ is the Hartree-Fock model in that subspace. Note that this wavefunction-oriented approach contrasts sharply with the density-oriented topological framework of the 'atoms in molecules' (AIM) method.¹⁸ The latter associates 'atoms' (or 'atomic basins,' sometimes lacking nuclei) with cellular regions of the electron density enclosed by 3-d spatial boundaries. Since known solutions of Schrödinger's equation exhibit no such boundaries (unless confined by physical barrier potentials), and since AIM specifically avoids reference to wavefunctions (and orbitals, hybridization, etc.), the

AIM 'atoms' lack an underlying $\hat{H}^{(0)}$ or wavefunction, but instead are defined by curvature conditions on the electron density surface. Despite these philosophical and mathematical differences, NPA and AIM methods display a surprising degree of correlation in many cases.¹⁹

3 NATURAL LOCALIZED ORBITALS

Each set of natural localized orbitals may be considered to lie along a sequence of transformations \hat{T} that leads from one-center basis AOs to final delocalized canonical MOs or NOs, viz.,



The initial transformation $\hat{T}_{AO \rightarrow NAO}$ is generally non-unitary (since basis AOs are generally nonorthogonal), but all remaining transformations ($\hat{T}_{NAO \rightarrow NHO}, \dots, \hat{T}_{NLMO \rightarrow MO}$) are unitary. Thus, each set of one-center (NAO, NHO), two-center (NBO), or semi-localized two-center (NLMO) orbitals constitutes a complete, orthonormal 'chemist's basis set' that can be employed to exactly represent any aspect of the calculation.

As a simple example, Figure 1 illustrates the successive stages of localization $MO \rightarrow NLMO \rightarrow NBO$ for formaldehyde (RHF/6-311G** level), showing the localization of the two inequivalent in-plane oxygen lone pairs of formaldehyde, the s-rich n'_O (left) and p-rich n''_O (right). Note that n''_O exhibits more pronounced delocalization than does n'_O (greater difference between the NLMO and its parent NBO), reflecting its stronger hyperconjugative interactions with the methylene moiety.

3.1 Natural Atomic Orbitals and Natural Population Analysis

The starting point for all NPA-related methods is determination of an optimal set of effective atomic orbitals for the molecular environment: the NAO basis set.¹⁶ These differ from free-space atomic orbitals (e.g., the analytic hydrogenic orbitals or the numerical Hartree-Fock orbitals of isolated atoms) in two important respects:

- (i) The effective partial charges of atoms in the molecular environment differ appreciably from those of free neutral atoms, so the NAOs are correspondingly more or less diffuse than free-atom NOs.
- (ii) The electron distributions at neighboring centers impose new boundary conditions on the long-range decay of the orbital, associated with steric (antisymmetry) constraints imposed by the Pauli exclusion principle. The NAOs therefore develop small nodal features near the cores of adjacent nuclei (fully analogous to the nodal feature of each valence orbital around its own core region) in order to prevent unphysical smooth penetration through regions occupied by electrons of adjacent nuclei. This consistent treatment of Pauli-orthogonality constraints is perhaps the single most important advantage of NAOs in serving as effective atom-like building blocks within the molecular environment.

Figure 2 illustrates the difference between the valence 2s NAO (top) and the corresponding s-type basis AOs (bottom)

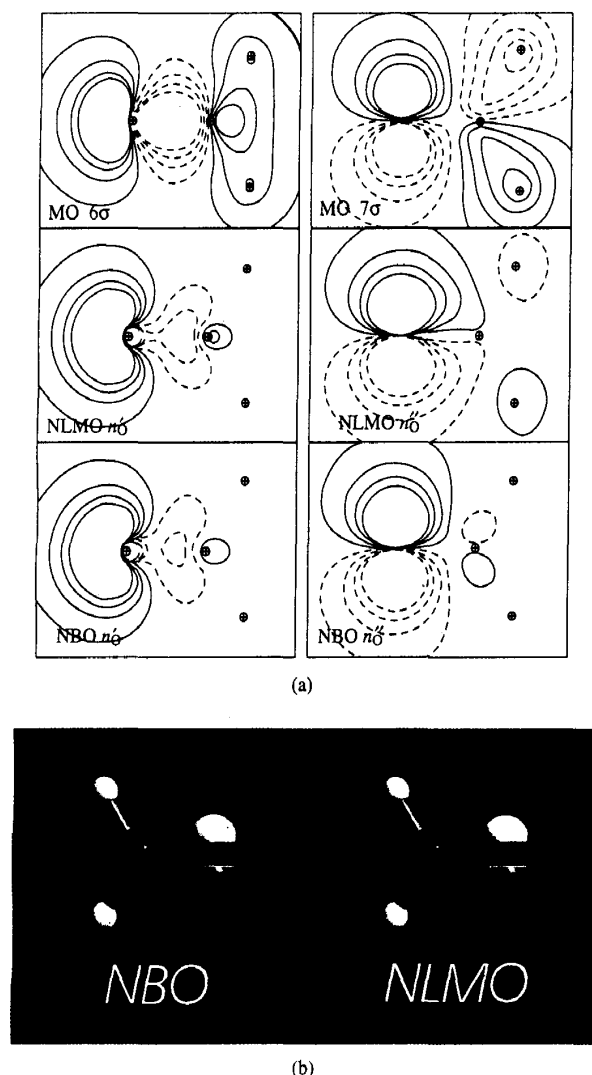


Figure 1 (a) Two-dimensional contour comparison of canonical MO (top), NLMO (middle), and NBO (bottom) for in-plane s-rich (n'_O , left) and p-rich (n''_O , right) oxygen lone pairs of formaldehyde (RHF/6-311G** level), showing the successive MO \rightarrow NLMO \rightarrow NBO degrees of localization. (b) Corresponding 'onion-skin' contour diagram, displaying differences between NBO vs. NLMO representation of oxygen lone pair n''_O in 3-d form

for the carbon atom of formaldehyde (RHF/6-311G**). As shown in the upper panel, the 2s NAO (solid line) differs from the corresponding spherically symmetric 'pre-NAO' (dashed line; Section 3.4) in the small nodal feature near the adjacent H atom that insures interatomic orthogonality (whereas the standard basis AOs lack all intra- and interatomic nodal features). While the idealized free-atom forms of pre-NAOs are suitable for visualizing orbital interactions (Section 3.4), only the orthonormal NAOs exhibit the realistic energetics of an 'atomic orbital' embedded in the actual steric environment of surrounding atoms.

3.1.1 NAO Algorithm

To find maximum-occupancy orbitals for atom A, one first finds the local eigenvectors $\tilde{\theta}_i^{(A)}$ of the one-center atomic block

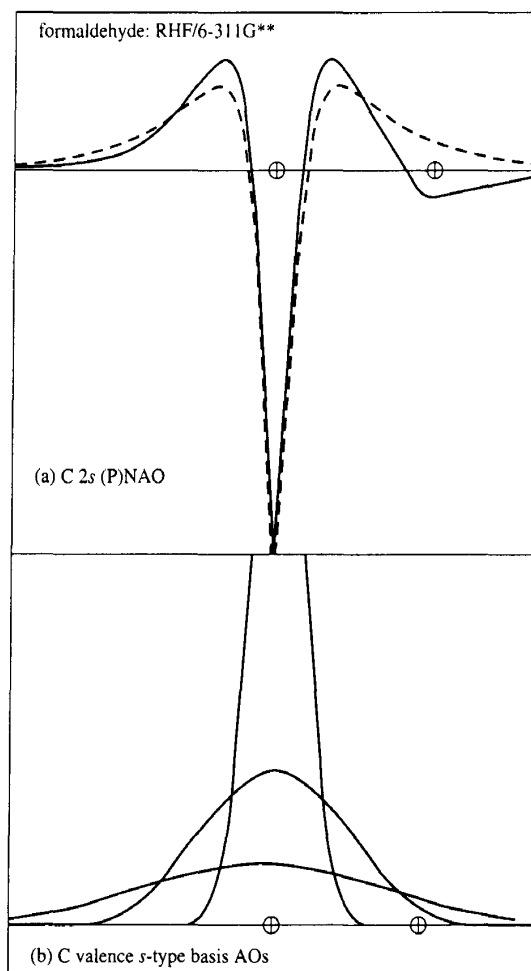


Figure 2 Carbon atomic orbitals in formaldehyde (RHF/6-311G** basis), plotted along the C-H bond axis, showing (a) the 2s NAO (solid) vs. non-orthogonal PNAO (dashed); (b) the three outermost s-type basis AOs of the 6-311G** basis set. Note the small nodal feature at the adjacent H that distinguishes the 2s NAO and PNAO, whereas Gaussian basis AOs lack nodal structure even in the core region of the C 1s electrons

$\hat{I}^{(A)}$ associated with basis AOs on atom A,

$$\hat{I}^{(A)} \tilde{\theta}_i^{(A)} = \tilde{q}_i^{(A)} \tilde{\theta}_i^{(A)} \quad (5)$$

If the starting basis orbitals lack unique atomic labels, it would first be necessary to calculate natural orbitals of each isolated atom in the full basis set, then reform the basis from the leading AOs on each center, but this step is usually unnecessary since use of AO basis sets is practically universal.

After the maximum-occupancy orbitals $\{\tilde{\theta}_i^{(A)}\}$ have been obtained for each atom A, it is necessary to restore full orthogonality. Whereas the maximum-occupancy and mutual-orthogonality properties are automatically achieved simultaneously for the M -center eigenorbitals of equation (1), the local eigenorbitals $\tilde{\theta}_i^{(A)}$ of equation (5) are mutually orthogonal on the same center ($\langle \tilde{\theta}_i^{(A)} | \tilde{\theta}_j^{(A)} \rangle = \delta_{ij}$), but non-orthogonal to orbitals on other centers ($\langle \tilde{\theta}_i^{(A)} | \tilde{\theta}_j^{(B)} \rangle \neq 0$ for $A \neq B$). Thus, the 'pre-orthogonal' orbitals $\tilde{\theta}_i^{(A)}$ (cf. Section 3.4) are next subjected to an occupancy-weighted symmetric orthogonalization

transformation, represented symbolically as

$$\hat{O}_{\text{OWSO}}\{\tilde{\theta}_i^{(A)}\} = \{\theta_i^{(A)}\} \quad (6)$$

This produces the final NAOs $\{\theta_i^{(A)}\}$ satisfying $\langle \theta_i^{(A)} | \theta_j^{(B)} \rangle = \delta_{AB} \delta_{ij}$ for all A, B and all i, j .

The precise form of \hat{O}_{OWSO} (and proof of its mathematical properties from the general Carlson–Keller theorem²⁰) is given in the original paper.¹⁶ As the name implies, the \hat{O}_{OWSO} transformation is related to Löwdin symmetric orthogonalization²¹ in maintaining ‘maximum resemblance’ between each $\tilde{\theta}_i^{(A)}$ and its orthogonalized counterpart $\theta_i^{(A)}$. However, the required degree of resemblance (integrated mean-square deviation) is not democratically enforced among all orbitals, but is rather weighted by the occupancy factor $\tilde{q}_i^{(A)} = \langle \tilde{\theta}_i^{(A)} | \hat{F} | \tilde{\theta}_i^{(A)} \rangle$ to favor orbitals that are most important in describing the actual electron density distribution. Thus, highly occupied orbitals are highly preserved in form, whereas orbitals of negligible occupancy are free to distort considerably. The \hat{O}_{OWSO} transformation virtually insures that the final NAOs are extremely stable to arbitrary basis set extensions (as is observed), whereas, e.g., the corresponding Löwdin orthonormal orbitals will all be symmetrically affected by any incremental extension of the basis set, no matter how small the actual contribution to describing the electron density distribution. Additional steps of the NAO algorithm (to guarantee rotational invariance, control numerical singularities associated with very small occupancies, etc.) are described in the original paper.

Figure 3 displays 2-d orbital profiles and 3-d surfaces of the carbon 2s, 2p, and 3d pre-NAOs of formaldehyde, illustrating their ‘textbook’ shapes and nodal features.

3.1.2 Natural Populations and Charges

Given the final orthonormal NAOs $\theta_i^{(A)}$, one can use equation (3) to rigorously compute their ‘natural’ populations $q_i^{(A)}$ (diagonal elements of the density operator in the NAO basis),

$$q_i^{(A)} = \langle \theta_i^{(A)} | \hat{F} | \theta_i^{(A)} \rangle \quad (7a)$$

which may be summed to give the total number of electrons N_A

$$N_A = \sum_i q_i^{(A)} \quad (7b)$$

and ‘natural charge’ Q_A on atom A (with atomic number Z_A)

$$Q_A = Z_A - N_A \quad (7c)$$

In accord with equations (4a, b), the natural populations $q_i^{(A)}$ necessarily satisfy the Pauli principle ($0 \leq q_i^{(A)} \leq 2$) and sum correctly to the total number of electrons ($\sum_A N_A = N$). Equations (7a–c) summarize ‘natural population analysis.’ (Some numerical NPA atomic charges for formaldehyde at correlated and uncorrelated levels will be presented in Section 4.2.)

Associated with their strong tendency to condense occupancy in the lowest few orbitals, the NAOs on each center A typically separate into two distinct sets: (i) the high-occupancy natural minimal basis (NMB) set, equal in number and type to the nominal minimal basis of occupied Hartree–Fock AOs in the atomic ground-state configuration, and (ii) the low-occupancy natural Rydberg basis (NRB) set, corresponding

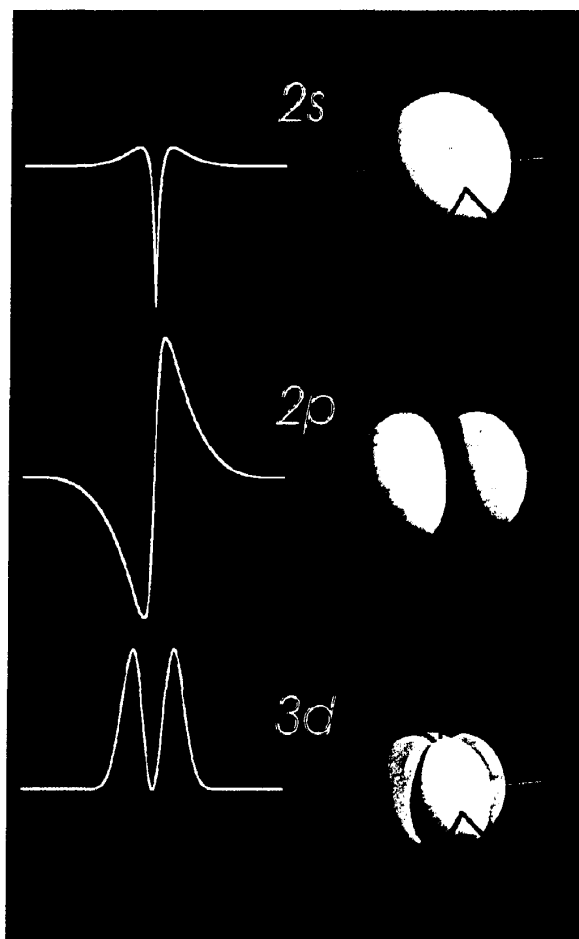


Figure 3 The 2s, 2p, and 3d pre-NAOs of the carbon atom in formaldehyde (RHF/6-311G** level), illustrating ‘textbook’ orbital shapes and nodal patterns

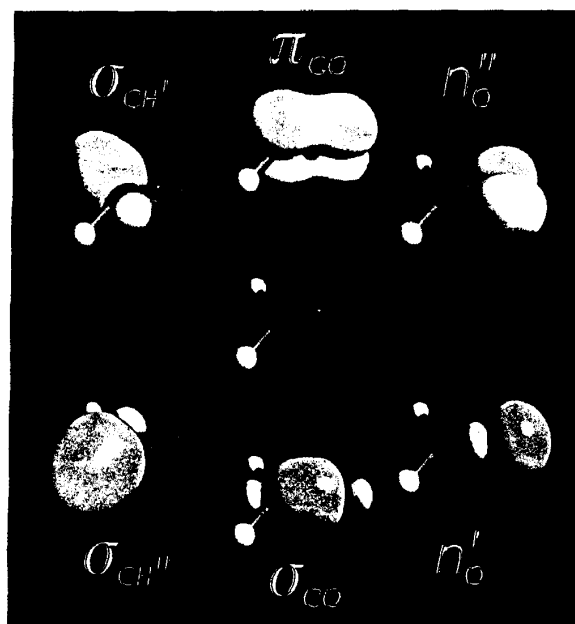
to all residual orbitals lying outside the formal valence shell. Occupancies of the NRB orbitals are commonly several orders of magnitude below those of the NMB set, in accordance with chemical intuition that their chemical role should be rather negligible. The NMB orbitals can in turn be separated into core and valence members, the former having practically full double occupancy, and the latter having occupancies corresponding closely to the expected valence-state configuration. Thus, the NAOs essentially recover from basis sets of arbitrary extension a simple chemical picture of minimal-basis-like simplicity, in close correspondence to the qualitative concepts of valence theory.

3.2 Natural Hybrid Orbitals and Natural Bond Orbitals

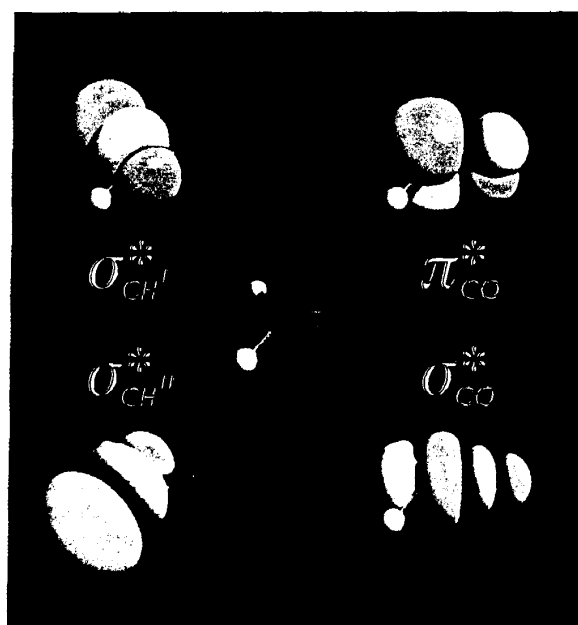
The chemist’s idealized Lewis structure picture describes the $N/2$ electron pairs as localized in one-center (‘lone pair’) or two-center (‘bond’) regions of the molecule. The natural bond orbital (NBO) algorithm^{12,15} leads to an optimal set of one- and two-center orbitals b_i that are in close correspondence with this picture. In effect, the algorithm searches the *density matrix* for the set of $N/2$ localized Lewis-type lone pair and bond orbitals of near-double occupancy that best describe the given wavefunction, with the residual weakly occupied non-Lewis-type

antibond and *Rydberg orbitals* representing small corrections due to delocalization. The natural Lewis structure wavefunction $\psi_L = \det|(b_1)^2(b_2)^2 \dots|$, with all Lewis-type orbitals doubly occupied, then forms a convenient perturbative starting point for describing electron delocalization effects in terms of weak departures from the idealized Lewis structure picture.

Figure 4 illustrates the principal valence NBOs of formaldehyde (RHF/6-311G**), showing the Lewis (upper) and non-Lewis (lower) pre-NBO forms. The highly



(a)



(b)

Figure 4 Valence-shell NBOs of formaldehyde (RHF/6-311** level), showing (a) Lewis-type ('donor') and (b) non-Lewis-type ('acceptor') orbital shapes and nodal patterns

recognizable and transferable character of these orbitals facilitates comparisons with other molecules having similar bonding features. (Additional numerical details of the NBOs for correlated and uncorrelated wavefunctions of formaldehyde are presented in Section 4.2.)

3.2.1 NHO/NBO Algorithm

To qualitatively sketch the NBO search algorithm, we start from the localized atomic ($\hat{r}^{(A)}$) and diatomic ($\hat{r}^{(AB)}$) subblocks of the partitioned density matrix \underline{d} in the NAO basis

$$\hat{r}^{(A)} = \underline{d}_{AA}, \hat{r}^{(AB)} = \begin{pmatrix} \underline{d}_{AA} & \underline{d}_{AB} \\ \underline{d}_{BA} & \underline{d}_{BB} \end{pmatrix} \quad (8)$$

for chosen atoms A, B. Each 1-center block $\hat{r}^{(A)}$ is first searched for 'lone pair' eigenvectors (n_A, n'_A, \dots) of occupancy ≥ 1.90 electrons (each such one-center function being subtracted from the density matrix as it is found, to prevent overcounting in the subsequent two-center searches). These one-center orbitals are identified as core ('CR', unhybridized core-type NAO) or valence lone pair ('LP') in the NBO output. The program next searches all two-center blocks $\hat{r}^{(AB)}$ for 'bond' eigenvectors (b_{AB}, b'_{AB}, \dots) of occupancy ≥ 1.90 e. In accordance with the bond-orbital formulation of Lennard-Jones²² each bond-type b_{AB} (labeled 'BD' in the NBO output) may be decomposed into its constituent normalized atomic hybrids (h_A, h_B) and polarization coefficients (c_A, c_B):

$$b_{AB} = c_A h_A + c_B h_B \quad (9)$$

Since an initial bond orbital b_{AB} found in the (A,B) block might slightly overlap, e.g., the bond orbital b_{AC} found in the (A,C) block, the algorithm systematically reorthogonalizes the hybrids (preserving maximum resemblance by the symmetric orthogonalization procedure²¹) to produce the final orthonormal set of natural hybrid orbitals (NHOs). If no satisfactory set of $N/2$ localized electron pairs is found in the initial search, the occupancy threshold, initially 1.90 e, is successively lowered in 0.1 e decrements down to 1.50 e and the entire search is repeated. (Alternatively, one may optionally extend the search to three-center blocks, looking for three-center bonds τ_{ABC} (labeled '3C' in the NBO output), as are necessary to describe bridge-bonding in boranes.) When a set of $N/2$ highly-occupied Lewis-type orbitals is found, each b_{AB} of the Lewis set is complemented by the corresponding antibond-type b_{AB}^* (labeled 'BD*' in the NBO output),

$$b_{AB}^* = c_B h_A - c_A h_B \quad (10)$$

and the span of the basis is finally completed with a residual set of Rydberg-type hybrids on each center (r_A, r'_A, \dots , labeled 'RY*' in the NBO output), chosen orthonormal to the previous hybrids and ordered by occupancy. The final NBO output displays the set of Lewis-type (unstarred) orbitals of highest total occupancy and reports the corresponding 'error' ρ_{NL}^* , the total occupancy of non-Lewis-type (starred) orbitals.

Figure 5 illustrates (in pre-NBO form) the A-H bonds σ_{AH} and antibonds σ_{AH}^* for first- and second-row AH_n hydride molecules, showing the related shapes of these orbitals and their expected smooth variations with position in the periodic table.

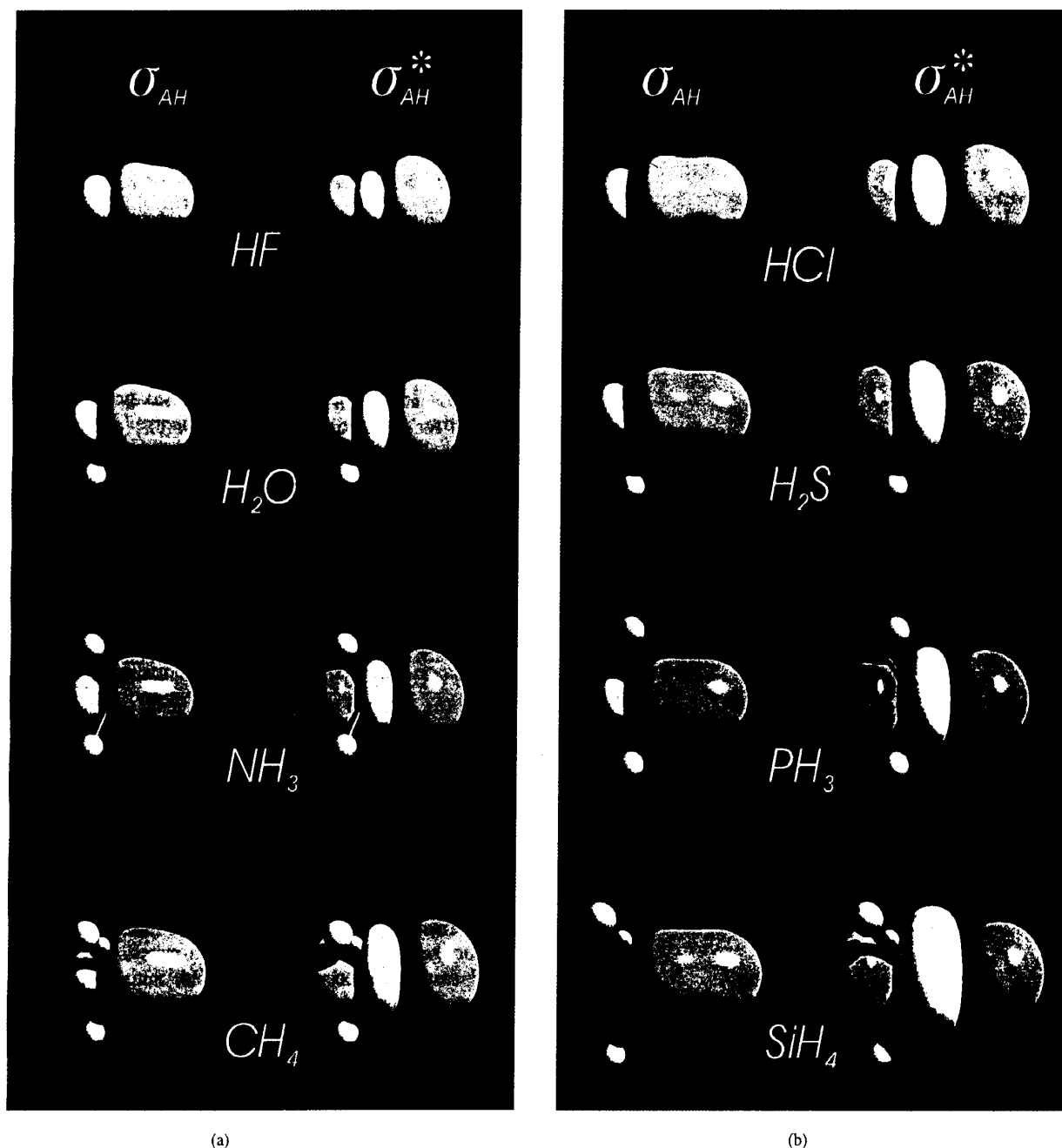


Figure 5 A-H bond (left) and antibond (right) NBOs for (a) first-row and (b) second-row AH_n hydrides (all at RHF-6-311G** level), showing the near-transferable forms and smooth variations with periodic position

3.2.2 Properties of Valence NHOs

Each valence NHO can be written as a generalized sp^v hybrid in terms of valence s, p NAOs (neglecting small corrections due to polarization functions)

$$h = n[s + v^{1/2}p_\theta] \quad (11)$$

where p_θ denotes a unit p-orbital (normalized linear combination of p_x , p_y , p_z) in direction θ . The hybrid p-character, $\%p = 100v/(1+v)$, varies from $v=0$ (0%p, 100%s) to $v=\infty$ (100%p, 0%s), and is generally found to be in excellent agreement with the predictions of *Bent's Rule*.²³ If h' , h'' denote two

NHOs on the same center, the orthogonality relation

$$\langle h' | h'' \rangle = n^2[(s|s) + (v'v'')^{1/2}(p_\theta | p_{\theta''})] = 0 \quad (12)$$

leads to the well-known relation²⁴ between hybrid direction and p-character,

$$\cos(\theta' - \theta'') = -(v'v'')^{-1/2} \quad (13)$$

which underlies many *VSEPR*-type structural rules. The NHO hybridizations are generally found to be in excellent agreement with the qualitative predictions of elementary valence theory with respect to both electronegativity and bond-angle changes,

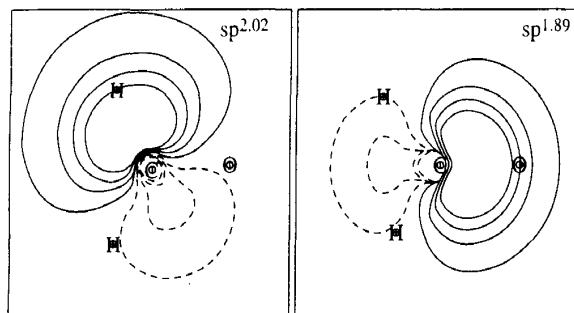


Figure 6 Two-dimensional orbital contour plots of the sigma-bonding carbon NHOs in formaldehyde (RHF/6-311G** level), showing the expected hybrid directionality along the C-H (left, $sp^{2.02}$) and C-O (right, $sp^{1.89}$) bonding axes

and they serve to quantify and extend numerous empirical correlations of this type.

Figure 6 illustrates the sp^2 -like NHOs of the carbon atom of formaldehyde (RHF/6-311G**), showing the $sp^{2.02}$ hybrid toward hydrogen (left) and the $sp^{1.89}$ hybrid toward oxygen (right), each exhibiting the expected directionality toward the bonded atom. Additional numerical details of the NHO hybridizations in correlated and uncorrelated treatments of formaldehyde are presented in Section 4.2.

As noted above (equations 9 and 10), each pair of valence NHOs h_A, h_B leads to a complementary pair of valence bond (b_{AB}) and antibond (b_{AB}^*) orbitals. Although the latter orbitals play no role in the elementary Lewis picture, their importance was emphasized by Lennard-Jones and Mulliken²⁵ in the treatment of homonuclear diatomic molecules. Since valence antibonds represent the residual atomic valence-shell capacity that is not 'saturated' by covalent bond formation, they are generally found to play the leading role in noncovalent interactions and delocalization effects beyond the Lewis structure picture. Indeed, it may be said that the NBO treatment of bond-antibond interactions constitutes its most unique and characteristic contribution toward extending the Lewis structure concepts of valence theory. Although the NBO hybrids and polarization coefficients are chosen to minimize the role of antibonds, the final non-zero weighting of non-Lewis orbitals reflects their essential contribution to wavefunction delocalization.

Confusion often arises between the virtual orbitals $\{\phi_i\}$ of SCF-MO theory and the localized valence antibonds $\{b_{AB}^*\}$. Although the spaces spanned by these sets overlap to a considerable extent, expansion of one set in terms of the other (e.g., in LCNBO-MO form) shows that they are far from identical. Indeed, the virtual orbitals are by their nature completely unoccupied, making no physical contribution to the SCF wavefunction or measurable properties. In contrast, the valence antibonds contribute irreducibly to the energy lowering and density shifts associated with electron delocalization, and their non-zero occupancies reflect the important physical effects of delocalization on the wavefunction and molecular properties.

3.2.3 Perturbative Analysis of NBO Donor-Acceptor Interactions

To see how valence antibonds contribute to the occupied molecular orbitals $\{\phi_i\}$ and orbital energies ε_i in Hartree-Fock

theory, it is useful to consider a simple perturbative treatment of the canonical Hartree-Fock equations:

$$\hat{F}\phi_i = \varepsilon_i\phi_i, \quad i = 1, 2, \dots, \text{occ} \quad (14)$$

If we examine these equations in the NBO basis-set representation, the NBO Fock matrix \underline{F} can be separated into diagonal and off-diagonal portions,

$$\underline{F}^{(0)} = \text{diag}(\underline{F}), \quad \underline{F}^{(1)} = \text{off-diag}(\underline{F}) \quad (15)$$

to serve as the 'unperturbed Hamiltonian' ($\underline{F}^{(0)}$) and 'perturbation' ($\underline{F}^{(1)}$) respectively. The occupied eigenfunctions of $\underline{F}^{(0)}$ are simply the Lewis-type NBOs $\{b_{AB}\}$, with eigenvalues $\varepsilon_{AB} = \langle b_{AB} | \hat{F} | b_{AB} \rangle$. A standard Rayleigh-Schrödinger perturbation treatment of the effect of mixing a doubly-occupied bond (say σ_{AB}^* , with orbital energy $\varepsilon_\sigma = \langle \sigma_{AB} | \hat{F} | \sigma_{AB} \rangle$) with an empty antibond (say σ_{CD}^* , with orbital energy $\varepsilon_{\sigma^*} = \langle \sigma_{CD}^* | \hat{F} | \sigma_{CD}^* \rangle$) leads to the estimated second-order energy lowering,

$$\Delta E_{\sigma \rightarrow \sigma^*}^{(2)} = -2 \frac{\langle \sigma_{AB} | \hat{F} | \sigma_{CD}^* \rangle^2}{\varepsilon_{\sigma^*} - \varepsilon_\sigma} \quad (16)$$

This familiar type of donor-acceptor ('2-e stabilizing') interaction is depicted schematically in Figure 7. Note that hyperconjugative $\sigma_{AB} - \sigma_{CD}^*$ attractions (equation 16) are usually opposed by repulsive $\sigma_{AB} - \sigma_{CD}$ 'steric' interactions in the same spatial region (cf. Section 5.3), so the net energy change of a given bonding arrangement involves a balance of competing terms.

The first-order wavefunction $\tilde{\phi}_{AB}$ associated with equation (16) manifests a weak delocalization tail:

$$\tilde{\phi}_{AB} = \mathcal{N} [\sigma_{AB} + \lambda \sigma_{CD}^*] \quad (17)$$

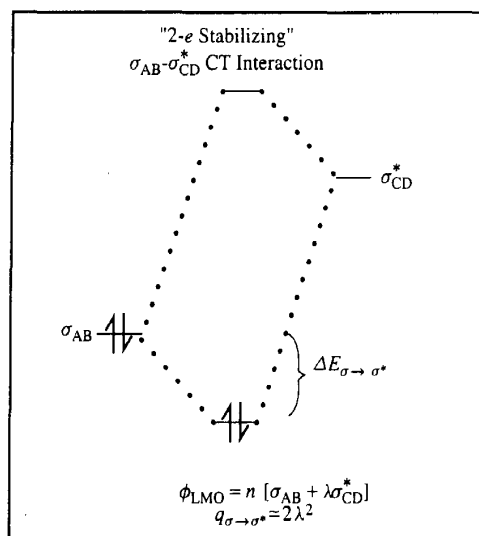


Figure 7 Schematic NBO perturbation diagram for '2-e stabilizing' interaction between a filled bond σ_{AB} and unfilled antibond σ_{CD}^* , leading to energy lowering $\Delta E_{\sigma \rightarrow \sigma^*}$.

with partial 'charge transfer' $q_{\sigma \rightarrow \sigma^*}$ from σ_{AB} to σ_{CD}^* , related to the perturbative mixing coefficient λ ,

$$q_{\sigma \rightarrow \sigma^*} = 2\lambda^2 = 2 \left(\frac{\langle \sigma_{AB} | \hat{F} | \sigma_{CD}^* \rangle}{\epsilon_{\sigma^*} - \epsilon_{\sigma}} \right)^2 \quad (18)$$

In this simple approximation, the occupancy of the Lewis-type donor orbital σ_{AB} is decreased to $2 - q_{\sigma \rightarrow \sigma^*}$, and that of the non-Lewis acceptor orbital σ_{CD}^* increased to $q_{\sigma \rightarrow \sigma^*}$, by the $\sigma_{AB} \rightarrow \sigma_{CD}^*$ charge delocalization. The high accuracy of the starting NBO Lewis structure makes these simple perturbative expressions quite useful for describing many aspects of electron delocalization in semi-quantitative fashion.

Figure 8 illustrates the hyperconjugative overlap of donor and acceptor NBOs for two simple examples: the $n_O'' \rightarrow \sigma_{CH}^*$ interaction of formaldehyde (left) and the vicinal antiperiplanar $\sigma_{CH} \rightarrow \sigma_{CH'}^*$ interaction of ethane (right), both treated at RHF/6-311G** level. It is evident that hyperconjugative interaction strength will depend sensitively on the relative orientation of donor and acceptor orbitals, leading to characteristic 'stereoelectronic' effects favoring coplanar *anti* alignments.

An interesting consequence of these perturbative formulas is seen by combining equations (16) and (18) in the form

$$|\Delta E_{\sigma \rightarrow \sigma^*}^{(2)}| = (\epsilon_{\sigma^*} - \epsilon_{\sigma}) q_{\sigma \rightarrow \sigma^*} \quad (19a)$$

Since $\epsilon_{\sigma^*} - \epsilon_{\sigma}$ is typically a large energy separation (of order unity in atomic units: 1 a.u. = 627.51 kcal mol⁻¹), this relationship can be rewritten as

$$|\Delta E_{\sigma \rightarrow \sigma^*}^{(2)}| \simeq q_{\sigma \rightarrow \sigma^*} \quad (\text{all in atomic units}) \quad (19b)$$

This implies that population changes as small as 0.001 e can correspond to energy lowerings of the order of 1 kcal mol⁻¹, and are hence 'chemically significant.' Thus, the reliability and stability of NAO/NBO populations at the milli-electron level of precision is critical to their general chemical usefulness.

3.3 Natural Localized Molecular Orbitals

Next in the sequence of transformations from localized to delocalized canonical orbitals is the 'semi-localized' set of natural localized molecular orbitals (NLMOs).²⁶ Although the NLMOs tend to closely resemble the more familiar Edmiston-Ruedenberg⁷ and Boys⁸ LMOs, they are obtained

by slightly modifying the NBOs rather than strongly modifying the canonical MOs, so as to take direct computational advantage of the localized NBO starting point.

Since Lewis-type NBOs typically have (slightly) less than double occupancy, they are not yet 'true' molecular orbitals in the Hartree-Fock sense. Equivalently, one may say that a determinant of doubly-occupied NBOs, the natural Lewis structure wavefunction $\Phi_L = \det |(\sigma_{AB})^2 (\sigma_{CD})^2 \dots|$ must have higher energy than the Hartree-Fock MO wavefunction

$$\Phi_{MO} = \det |(\phi_1)^2 (\phi_2)^2 \dots| \quad (20a)$$

owing to the omission of delocalization effects such as represented in equation (17). Nevertheless, when transformed into the NBO basis, the density matrix is of very nearly diagonal form, with diagonal elements of nearly 2 for each Lewis-type (unstarred) NBO and nearly 0 for each non-Lewis-type (starred) NBO, and with only small off-diagonal elements connecting the starred and unstarred blocks. Thus, a sequence of 2×2 Jacobi rotations can be used to zero these connecting off-diagonal elements, bringing the trace of the unstarred block to N and that of the starred block to 0. At this point, the transformed orbitals $\tilde{\phi}_i$ must each have occupancy = 2 in the unstarred (occupied) block and 0 in the starred (virtual) block. They are hence true molecular orbitals in the sense that

$$\Phi_{LMO} = \det |(\tilde{\phi}_1)^2 (\tilde{\phi}_2)^2 \dots| \quad (20b)$$

is precisely the same wavefunction as equation (20a), except for a possible trivial phase factor.

As remarked above, the final NLMOs $\{\tilde{\phi}_i\}$ are found to be rather similar in form to Edmiston-Ruedenberg or Boys LMOs, but they enjoy several numerical and conceptual advantages: (i) they are more efficiently calculated, since the starting NBOs (obtained very economically) require relatively few Jacobi rotations to achieve the necessary slight delocalization (cf. Figure 1), compared with the much larger number needed to bring the canonical MOs to semi-localized form. (ii) The occupied and virtual blocks are localized simultaneously, with no increased computational cost. (iii) The NLMO procedure applies, virtually without modification, to more general correlated wavefunctions, although in this case the diagonal elements of unstarred and starred blocks are not reduced precisely to 2 and 0 respectively. Other differences (involving description of inequivalent lone pairs, sigma-pi separation, etc.) are beyond the scope of the present article.

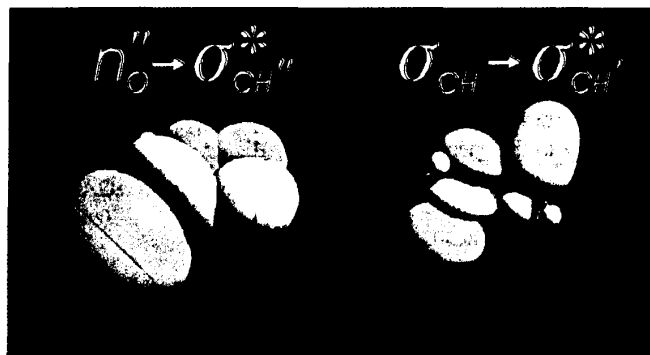


Figure 8 Three-dimensional PNBO overlap diagrams depicting hyperconjugative interactions for the in-plane $n_O'' \rightarrow \sigma_{CH}^*$ interaction of formaldehyde (left) and the vicinal antiperiplanar $\sigma_{CH} \rightarrow \sigma_{CH'}^*$ interaction of ethane (right), both at RHF/6-311G** level

From the mode of construction, it is evident that each NLMO will have a dominant contribution from a 'parent' Lewis-type NBO σ_{AB} , with weaker contributions (delocalization tails) from non-Lewis-type NBOs σ_{CD}^* , leading to expressions of the form

$$\tilde{\phi}_{AB} = \mathcal{N} [\sigma_{AB} + \lambda \sigma_{CD}^* + \dots] \quad (21)$$

The numerical form of the NLMO thus closely mimics the perturbative expression (17), which may be taken to 'explain' the delocalization tails.

It is important to emphasize that the bond-antibond interactions depicted in equation (17) or equation (21) are the only physically significant delocalizations in Hartree-Fock theory. The remaining symmetry adaptation that converts LMOs into MOs (i.e., that converts equation 20b into equation 20a) is only 'decorative,' with no physical effect on the HF wavefunction or other measurable property.

3.4 Pre-orthogonal Localized Orbitals: Overlap and Interaction Strength

Although orthonormality is maintained in the construction of NAOs, for conceptual purposes it is convenient to consider the associated 'pre-orthogonal' orbitals (PNAOs) that differ only in omission of the final interatomic orthogonalization step of equation (6), as shown in Figure 2. These PNAOs exhibit the familiar free-atom symmetries of textbook atomic orbitals (see Figure 3), and their overlaps vividly suggest the strength of orbital interaction in the actual NAO matrix elements, in accordance with Mulliken-type approximations.²⁷

By merely replacing NAOs with PNAOs, while retaining all other details of the orbital transformations, one similarly obtains the corresponding pre-NBOs (PNBOs) and pre-NLMOs (PNLMOs). Thus, NAO/NBO graphics representations are normally constructed from such pre-orthogonal precursors (e.g., Figures 3–8), so that one retains the advantages of overlapping orbitals for visualization purposes, but avoids their rather severe formal and numerical pathologies²⁸ in the actual numerical work.

3.5 Open-shell NBOs and Maximum Spin-paired NBOs

For open-shell systems, where 1-electron density matrices for α and β spin sets are no longer equivalent, it is straightforward to analyze each spin density separately for the distinct hybrids and Lewis structures of opposite spin.²⁹ This emphasizes that the NBO Lewis structure concept refers to a particular localized bonding pattern of one- and two-center interactions rather than to electron pairing per se. Since Coulomb and exchange interactions for α and β electrons differ appreciably in open-shell systems, the associated spin polarization effects are most naturally described in terms of 'different Lewis structures for different spins,' the default NBO procedure.

However, as suggested by Michl and co-workers,³⁰ it may also be useful to develop a picture of radical spin polarization starting from 'maximum spin-paired NBOs' (MSPNBOs), in which α and β electrons are assumed to be paired in the same spatial NBO, prior to spin polarization. For this purpose, the α and β spin density matrices are initially averaged:

$$\hat{r}^{av} = \frac{1}{2}(\hat{r}^\alpha + \hat{r}^\beta) \quad (22)$$

and this spin-averaged density is used to obtain MSPNBOs by the usual closed-shell NBO algorithm. Although the non-Lewis error ρ_{NL}^* of MSPNBO description is higher, such orbitals can often be related more directly to those of a parent spin-paired species, permitting radical formation, spin polarization, and spin-orbit coupling to be analyzed in greater detail.

4 NATURAL LOCALIZED CONFIGURATIONS

An N -e configuration of NBOs provides a starting point for describing the N -electron state function of the system in localized bonding terms. Although the single 'natural Lewis structure' configuration is an excellent approximation for saturated ground-state systems, it cannot generally represent highly delocalized systems with satisfactory accuracy. Nevertheless, in favorable cases it may suffice to employ a small number of localized configurations ('diabatic precursor states') to describe the final ('adiabatic') delocalized state function in compact form.

Although such a multi-configurational wavefunction of localized orbitals is sometimes associated with 'electron correlation,' it is important to realize that the delocalized wavefunction may (or may not) be representable as a single determinant of delocalized orbitals, i.e., as an uncorrelated SCF-MO wavefunction. Thus, the irreducible contribution of two or more localized Lewis (resonance) structure configurations in the state function (or density matrix) carries no direct implication for the degree of electron correlation. It is also important to realize that a localized configurational description might apply at the density matrix level (incoherent superposition) rather than the wavefunction level (coherent superposition). This is the starting point for the NRT formalism discussed in Section 4.1. Other aspects of the NBO/NRT description of electron correlation and delocalization are summarized in Section 4.2, and a multi-configurational CAS/NBO procedure for incorporating localized correlation effects is described in Section 4.3.

4.1 Natural Resonance Theory

The single Lewis-structure picture is often inadequate to describe the delocalized form of the wavefunction (and associated density \hat{r}). It is therefore useful, following Pauling,³¹ to picture the actual system as a 'resonance hybrid' composed of contributions from several such localized Lewis 'resonance' structures r , with associated localized densities $\hat{r}^{(r)}$. A general goal of such theories is to describe the molecular properties $\langle \hat{M} \rangle$ of the actual delocalized system in terms of a weighted average of the corresponding properties $\langle \hat{M} \rangle_r$ of idealized resonance structures,

$$\langle \hat{M} \rangle = \sum_r^{RS} w_r \langle \hat{M} \rangle_r \quad (23a)$$

with non-negative 'resonance weights' w_r summing to unity.

The starting point for an alternative formulation of resonance theory is recognition that the necessary and sufficient condition for any one-electron system property $\langle \hat{M} \rangle$ to be representable in the resonance hybrid form (equation 23a) is given by an equation involving localized densities (incoherent

superposition) rather than wavefunctions (coherent superposition), viz.

$$\hat{r} = \sum_r^{RS} w_r \hat{r}^{(r)} \quad (23b)$$

From the Hellmann–Feynman theorem, one can show that the 1-e operators covered by conditions (23a,b) include molecular geometry³² as well as electron density, dipole moment, kinetic energy, and other important properties. Moreover, at the uncorrelated Hartree–Fock level all properties are formally covered by this condition. Hence, condition (23b) is a rather general prerequisite for the validity of resonance theory, and is taken as the starting point for the ‘natural’ resonance theory (NRT).³³ Note that the terms included in equation (23b) have no necessary connection to the Rumer diagrams underlying Pauling’s original resonance wavefunction ansatz.³⁴

4.1.1 NRT Variational Algorithm

It is generally possible to associate a given NBO donor–acceptor interaction (cf. Figure 7) with an equivalent resonance structure diagram, as illustrated in Figure 9. This figure shows how the formal 2-e transfer corresponding to a vicinal $\sigma_{AB} \rightarrow \sigma_{CD}^*$ NBO interaction leads to the ‘double-bond no-bond’ resonance structure shown in the lower-right panel. Similar associations allow a table of NBO interactions (such as generated in second-order perturbative analysis; Section 3.2.3) to be converted into a corresponding list of candidate resonance structures for inclusion in equations (23a,b).

Given the bonding pattern for a particular resonance structure r , one can use a restricted NBO procedure (‘directing’ the search for the specified pattern) to form the idealized density

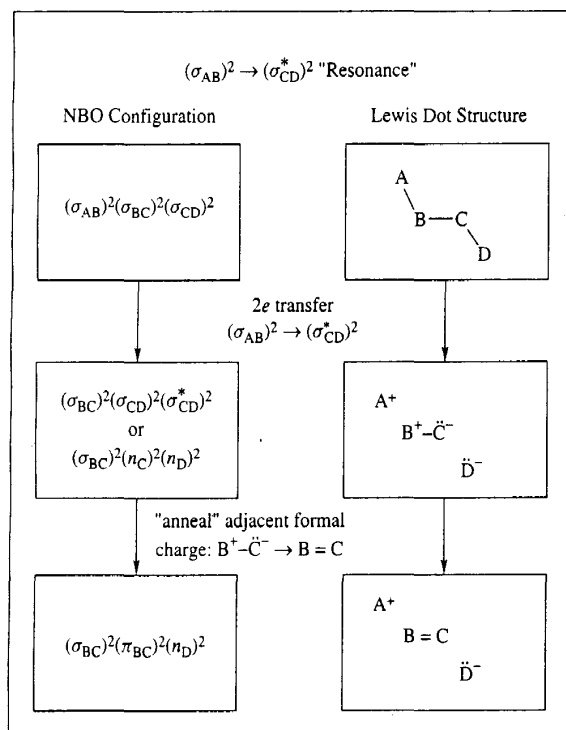


Figure 9 Schematic association of $\sigma_{AB} - \sigma_{CD}^*$ NBO interaction (cf. Figure 7) with the ‘double-bond no-bond’ resonance structure

operator $\hat{r}^{(r)}$ for the associated natural Lewis structure wavefunction. The optimal weights $\{w_r\}$ to satisfy criterion (23a, b) can be determined from the NRT least-squares variational functional,

$$\Delta(\{w_r\}) = \min_{\{w_r\}} \left\| \hat{r} - \sum_r^{RS} w_r \hat{r}^{(r)} \right\| \quad (24)$$

where $\|\hat{O}\|^2 = \text{Tr}(\hat{O}^2)$ is the operator norm. If Δ_{NBO} denotes the value of $\Delta(\{w_r\})$ when the summation in equation (24) is restricted to the single best NBO structure, one can assess the accuracy of the NRT description in terms of the fractional improvement $f(\{w_r\})$:

$$f(\{w_r\}) = \frac{\Delta_{\text{NBO}} - \Delta(\{w_r\})}{\Delta_{\text{NBO}}} \quad (25)$$

which varies between 0 (no improvement over the single-term NBO description) and 1 (exact satisfaction of equations 23a,b). Thus, variational minimization of equation (24) provides both optimal NRT weightings $\{w_r\}$ as well as an intrinsic criterion, $0 \leq f(\{w_r\}) \leq 1$, for the accuracy of the NRT description.

In principle, the full NRT variational procedure (equation 24) would require numerically intensive matrix transformations of all possible $\hat{r}^{(r)}$ s to a common basis set (e.g., NAOs) as well as simultaneous storage of these matrices during the search for the global minimum of the multi-dimensional $\{w_r\}$ -surface (e.g., by the method of simulated annealing). This rapidly presents intractable numerical and storage problems if reasonable numbers of resonance structures (n_{RS}) are admitted for larger systems of chemical interest. However, dramatic numerical simplifications are possible in the limit of a single dominant ‘reference’ structure, where the resonance weightings are increasingly dictated by population changes among the NBOs (rather than changes in the form of the NBOs) which can be efficiently treated for large n_{RS} . The actual NRT numerical algorithm is therefore a composite of two steps: (i) the full-dimensional procedure (equation 24) for the relatively small number of reference structures (n_{ref}), and (ii) the simplified population-weighting procedure for the large manifold of secondary structures associated with each ‘parent’ reference structure. (Further details of each step are beyond the scope of this article.) The composite NRT strategy allows a high level of chemical detail (including hundreds of possible resonance structures) to be described within practical computational limits.

Since the calculated NRT weightings depend somewhat on the chosen number of reference structures, discontinuities in NRT bond indices may result from changes in the reference set. By default, the reference set is chosen to include all structures whose weightings are at least $0.35w_{\text{largest}}$, and the NRT optimizations are repeated iteratively until this condition is achieved. Since NRT weightings are employed primarily for comparative purposes, the number and type of reference structures may be chosen specifically with respect to the actual comparisons that are desired. For example, to describe a *potential energy surface* along a particular reaction coordinate, one would specify that both reactant-like and product-like resonance structures be treated as reference structures throughout the reaction path (even in regions where one or the other would fall below the default threshold) to insure completely smooth changes of NRT weightings over the entire reaction coordinate. Control of the reference set can extend the range of variations

and level of detail considerably beyond that treated by the default NRT procedure.

4.1.2 Natural Bond Order and Valency

From the NRT resonance weights w_r and number of A-B bonds $P_{AB}^{(r)}$ in resonance structure r , one can determine the natural bond order P_{AB} between atoms A and B as the resonance-weighted average,

$$P_{AB} = \sum_r^{RS} w_r P_{AB}^{(r)} \quad (26)$$

By summing all the formal bond orders to atom A, one can similarly determine the natural valency V_A of atom A,

$$V_A = \sum_B^{\text{atoms}} P_{AB} \quad (27)$$

The natural valencies are found to closely resemble the classical valency values associated with position in the periodic table ($V_H = 1$, $V_C = 4$, $V_N = 3$, etc.). Similarly, the natural bond orders closely resemble those expected from classical structural formulas, whether the bonding is of covalent, coordinate, or ionic type. In both respects, the NRT quantities conform more closely to classical valence concepts than do the analogous MO (Coulson) bond order, Wiberg bond index, or similar MO-related bond indices (see Section 6.1). Illustrative numerical NRT results for formaldehyde in correlated and uncorrelated levels are presented in Section 4.2.

A significant difference should be noted between Pauling's treatment of 'valence bonds' and the corresponding NRT description of polar covalent or ionic bonding. In Pauling's formulation each polar bond requires two distinct resonance structures for its depiction, one 'covalent' and one 'ionic.' However, in the NRT framework each localized 2-center electron pair is represented as a bond-line of a single resonance structure, whether the bond is polar ($c_A \neq c_B$) or nonpolar ($c_A = c_B$). Avoidance of covalent-ionic resonance in the NRT framework greatly reduces the number of NRT resonance structures required in expansions such as equation (26).

To draw a closer correspondence to the older resonance terminology of covalent-ionic resonance, one can use the difference in bond polarization coefficients c_A , c_B as an intrinsic measure of ionicity (i_{AB}) of an A-B bond,

$$i_{AB} = \left| \frac{c_A^2 - c_B^2}{c_A^2 + c_B^2} \right| \quad (28)$$

which varies from purely covalent ($i_{AB} = 0$) to purely ionic ($i_{AB} = 1$). With the associated $i_{AB}^{(r)}$ for structure r , each $P_{AB}^{(r)}$ can be partitioned into 'covalent' and 'electrovalent' components ($P_{AB}^{(r)} = c_{AB}^{(r)} + e_{AB}^{(r)}$, where $c_{AB}^{(r)} = P_{AB}^{(r)}(1 - i_{AB}^{(r)})$, $e_{AB}^{(r)} = P_{AB}^{(r)}i_{AB}^{(r)}$). This leads, through equation (26), to a formal decomposition of total NRT bond order into covalent and electrovalent (or 'ionic') contributions,

$$P_{AB} = c_{AB} + e_{AB} \quad (29a)$$

Similarly, total atomic valency V_A is expressed as a sum of 'covalency' (C_A) and 'electrovalency' (E_A),

$$V_A = C_A + E_A \quad (29b)$$

These equations allow one to connect NRT bond order (P_{AB}) with Pauling-Wheland bond order (c_{AB}) and the older covalent-ionic resonance concepts. They also allow smooth integration of resonance and valency concepts for organic and inorganic compounds.

The natural bond orders are found to exhibit excellent correlations with molecular geometry, as expected from classical bond order-bond length (P_{AB} - R_{AB}) relationships. These relationships are approximately linear in regions associated with positive integer bond orders, but become logarithmic in the asymptotic limit $R_{AB} \rightarrow \infty$ (as required on physical grounds). The utility of such correlations is found to be maintained as bond polarity is varied, leading to unified treatment of covalent and ionic bonding across a wide range of chemical species.

4.2 Localized and Delocalized Aspects of Electron Correlation

Although the NRT formalism formally represents a delocalized system in terms of multiple Lewis structures (each with an associated NBO configuration), in principle such resonance delocalization effects are not intrinsically 'multi-configurational' in the electron correlation sense. Indeed, NRT analysis applies in virtually unmodified form to single-configurational SCF as well as to multi-configurational (MC) SCF or configuration interaction (CI) wavefunctions that incorporate electron correlation, often with little change in delocalization patterns. Nor does inclusion of electron correlation intrinsically conflict with the localized Lewis-like picture, for the leading post-HF corrections are expected to be associated with electron pairs (of opposite spin) confined to the same spatial region and hence essentially localized and Lewis-like. For example, the correlation corrections of the *generalized valence bond* (GVB) wavefunction are defined with respect to a single Lewis structure (spin-pairing) pattern, whereas resonance-type delocalization is incorporated by allowing GVB orbitals of each spin pair to delocalize self-consistently over other atoms. Thus, electron correlation and delocalization are not inherently related. However, electron correlation can be expected to alter the SCF-level delocalization patterns in a characteristic manner.

NBO analysis provides a useful classification of electron correlation contributions, allowing the familiar correlation 'types' of diatomic molecules (left-right, in-out, angular)³⁵ to be recognized in the polyatomic framework. In accordance with the GVB picture, one expects that the leading correlation terms are of intra-bond character, correcting for the improper HF description of chemical bond dissociation. Such correlations appear as enhanced σ_{AB} - σ_{AB}^* interactions, corresponding to differential left-right polarization of α and β spin orbitals within the A-B bonding region. The leading dynamical correlations are similarly of intra-pair character, associated with increased occupancy of extra-valence-shell Rydberg orbitals r_A , r_B describing radial and angular correlations of the A-B electron pair.

However, electron correlations are also found to characteristically enhance inter-bond (inter-pair) interactions, including those between distinct molecular species. The best known terms of this type are associated with the weak London dispersion interactions between closed-shell atoms. However, significantly stronger inter-bond correlation effects are possible when strong σ_{AB} - σ_{CD}^*

delocalization is present, as can be anticipated from a simple physical picture: it was previously noted (cf. also Sections 5.3 and 5.4) that stabilizing $\sigma_{AB}-\sigma_{CD}^*$ donor-acceptor interactions are generally in competition with destabilizing $\sigma_{AB}-\sigma_{CD}$ steric repulsions in the same region of space, so that favorable polarization of σ_{CD}^* toward σ_{AB} (and correspondingly, of σ_{CD} away from σ_{AB}) is needed for net energy lowering. However, when the electrons are correlated, such spin-orbital polarization can occur differentially and dynamically for electrons of α and β spin. Each spin set thereby gains enhanced $\sigma_{AB}-\sigma_{CD}^*$ donor-acceptor attraction (and reduced $\sigma_{AB}-\sigma_{CD}$ repulsion) without net polarization changes of the C-D bond pair. Such dynamic polarization effects may be referred to as 'correlation-enhanced delocalizations' to suggest their role in enhancing donor-acceptor interactions that are already present at the uncorrelated SCF level. Note that such correlation-enhanced donor-acceptor interactions can be much larger than conventional dispersion attractions between analogous atomic species (i.e., between isoelectronic closed-shell atoms, lacking residual valence-shell acceptor orbitals). This parallels the situation for molecular intra-pair correlations, where dynamical left-right bond polarization provides a fundamentally new correlation mechanism that is unavailable to atoms.

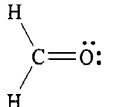
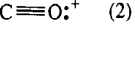
Table 1 illustrates some characteristic effects of electron correlation on the NPA/NBO/NRT descriptions of formaldehyde. The table compares uncorrelated HF analysis with corresponding complete active space multi-configurational (CASSCF), second-order Møller-Plesset perturbation theory (MP2), and hybrid density functional (B3LYP) treatments, all at the 6-311G** basis level with optimized RHF geometry. It can be seen that correlation leads to significantly less polar π_{CO} bond (with resulting changes in C, O natural charges) and to enhanced $n_O' \rightarrow \sigma_{CH}^*$ delocalization (as reflected in reduced population of n_O' , increased population of σ_{CH}^* , and enhanced NRT weighting of secondary resonance structures). Although the three correlated descriptions are qualitatively similar, several differences distinguish B3LYP from the CASSCF and MP2 treatments (e.g., the negligible σ_{CO}^* and π_{CO}^* occupancies, contrary to the expected pattern of dynamic left-right correlations). Note that in the DFT case, the availability of the Kohn-Sham effective 1-e Hamiltonian operator yields additional energetic details of electron correlation through second-order NBO perturbative analysis (Section 3.2.3).

4.3 CAS/NBO Wavefunctions

Although NBOs are most commonly used to analyze a given wavefunction, they may also be used to improve the computation of wavefunctions, particularly with respect to inclusion of electron correlation. Considerable evidence suggests that correlation effects are most efficiently described in terms of localized orbitals.³⁶

NBOs have been used as starting active-space orbitals in CASSCF calculations, leading to rather remarkable solutions describing localized correlation effects.³⁷ The only modification of conventional CASSCF is to replace the initial guess MOs (or NOs) by NBOs, so the active space is defined in terms of a starting NBO configuration. This can be accomplished with 'checkpointing' options that store the NBOs from an earlier HF calculation in the location where the post-HF procedure expects to find MOs. The acronym 'CAS/NBO' distinguishes the NBO-based procedure from conventional MO-based methods.

Table 1 Summary of NPA, NBO, and NRT Analysis for Formaldehyde

	RHF	CASSCF	MP2	B3LYP
Natural charges				
C	0.3896	0.3278	0.2848	0.2832
O	-0.5657	-0.4508	-0.4508	-0.4800
H	0.0880	0.0615	0.0830	0.0984
Natural bond orbitals				
σ_{CH}	h_C	$sp^{2.01}$	$sp^{2.01}$	$sp^{2.00}$
	h_H	s	s	s
	%pol.	55.68	55.00	55.91
	occ.	1.9940	1.9796	1.9681
σ_{CO}	h_C	$sp^{1.89}$	$sp^{1.91}$	$sp^{1.92}$
	h_O	$sp^{1.41}$	$sp^{1.52}$	$sp^{1.53}$
	%pol.	33.94	34.11	33.86
	occ.	1.9995	1.9807	1.9723
π_{CO}	h_C	p	p	p
	h_O	p	p	p
	%pol.	32.79	34.90	35.54
	occ.	2.0000	1.9363	1.9382
n_O'	h_O	$sp^{0.70}$	$sp^{0.65}$	$sp^{0.67}$
	occ.	1.9895	1.9839	1.9649
n_O''	h_O	p	p	p
	occ.	1.9080	1.8593	1.8537
σ_{CH}^*	occ.	0.0459	0.0801	0.0736
σ_{CO}^*	occ.	0.0000	0.0219	0.0239
π_{CO}^*	occ.	0.0000	0.0634	0.0516
Natural resonance theory				
	95.15%	91.86%	91.35%	93.90%
$H: -$				
 (2)	4.52%	7.10%	6.76%	6.10%
Others	0.34%	1.04%	1.88%	0.00%
Natural bond order				
CO	2.0452	2.0710	2.0677	2.0610
CH	0.9741	0.9541	0.9473	0.9695
Natural atomic valency				
C	3.9933	3.9793	3.9623	4.0000
O	2.0452	2.0710	2.0677	2.0610
H	0.9741	0.9541	0.9473	0.9695

Comparing uncorrelated Hartree-Fock (RHF) with correlated multi-configurational (CASSCF) - complete valence-shell CASSCF(12,10), 13860 configurations - second-order Møller-Plesset (MP2), and hybrid density functional (B3LYP) results, all at 6-311G** basis level and RHF optimized geometry. NBO entries include the hybrid type (h_A, h_B), %-polarization on the first-named atom ($100c_A^2$), and occupancy (orbital population, in e).

As usual, the CAS wavefunction incorporates complete CI over a chosen number of electrons (N) and orbitals (M) that constitute the active space [CAS(N,M)], with iterative self-consistent optimization of all occupied and partially occupied orbitals. Compared with conventional CAS/MO, the following advantages of CAS/NBO may be noted:

- (i) In general, a smaller NBO active space can be selected, clearly identified with the structural features of interest. For example, study of a particular A–B bond-breaking process would require only the directly involved σ_{AB} , σ_{AB}^* NBOs to be included, leading to a compact CAS(2,2) ‘HOMO–LUMO-like’ treatment.
- (ii) CAS/NBO procedures appear to have significantly improved convergence characteristics, leading to satisfactory solutions in many cases where CAS/MO fails entirely.
- (iii) The final CASSCF orbitals are often found to be similar in form to the initial NBOs, requiring less orbital reorganization to achieve self-consistency than in the MO case. This indicates that NBOs are already good ‘correlating orbitals.’
- (iv) In many cases, entirely new types of CAS solutions can be found which retain the essentially localized character of the starting NBOs. It is therefore possible to treat correlation effects locally and selectively, taking advantage of the approximate additivity of correlation contributions from distinct bonding regions (‘divide and conquer’ strategy).
- (v) Consistent with the picture of correlation in diatomic molecules, one can select active-space NBOs that correspond specifically to left–right, in–out, or angular correlations for the chosen bonding region, to further isolate distinct correlation contributions.

The CAS/NBO procedure was employed to demonstrate, e.g., that correlation effects in the two aldehyde groups of malonaldehyde (CHOCH2CHO) can be independently treated in a manner similar to isolated formaldehyde. Localized CAS is also useful in describing systems where two or more localized ‘diabatic precursor’ configurations contribute to the adiabatic potential energy surface, such as the interesting double-well 2^1A_1 excited state of formaldehyde.³⁸

5 LOCALIZED NAO/NBO ANALYSIS OF ENERGY AND OTHER MOLECULAR PROPERTIES

The natural localized orbital transformations provide useful tools for analyzing various molecular properties or energy ‘components’ in localized bonding terms. We briefly summarize the underlying principles of several such analyses that are implemented in the general NBO program, restricting attention primarily to HF-level treatment.

5.1 NBO Energetic Analysis: \$DEL Deletions

In addition to the second-order perturbative analysis (Section 3.2.3), it is possible to perform a complementary energetic analysis of a HF wavefunction by ‘deleting’ certain orbitals (or their specific interactions with other orbitals) and recalculating the approximate SCF energy E_{dele} for a hypothetical system with such interactions absent. The resultant energy change,

$$\Delta E_{\text{dele}} = E_{\text{full}} - E_{\text{dele}} \quad (30)$$

measures the loss of stabilization (variational energy raising of E_{dele} relative to E_{full}) associated with the deleted interactions. By re-optimizing the geometry with respect to E_{dele} , one can also determine the detailed structural consequences of

the deleted interaction(s). Through selective deletions and re-optimizations, it is often possible to identify the electronic origin of specific structural effects in terms of specific NBO Fock matrix elements.

If E_{dele} represents the effect of deleting a single $\sigma \rightarrow \sigma^*$ NBO interaction, ΔE_{dele} may be directly compared (usually, within $\approx 10\%$ accuracy) with the simple second-order estimate $\Delta E_{\sigma \rightarrow \sigma^*}^{(2)}$, equation (16). However, for multiple deletions, ΔE_{dele} incorporates higher-order coupling effects that are ignored in the sum of corresponding second-order estimates. In an important limiting case, one can delete all non-Lewis acceptor orbitals (NOSTAR deletion) to evaluate the energy:

$$E_L = E_{\text{dele}}(\text{NOSTAR}) = \langle \psi_L | \hat{F} | \psi_L \rangle \quad (31)$$

of the idealized natural Lewis structure wavefunction ψ_L of doubly-occupied Lewis-type NBOs. The approximate energetic effects of deletions are evaluated by a ‘single pass’ procedure using the converged Fock operator \hat{F} of the full calculation. This is numerically efficient, but leads to a slight self-consistency error in the Coulomb and exchange operators, and thus to slightly non-variational energetics, owing to the small (usually $\ll 1\%$) rearrangements of electron density that accompany the deletion. Hence, E_{dele} is most reliable when the associated population shifts are small compared with the total electron density, i.e., when the deletions involve small numbers of weakly occupied NBOs, NHOs, or NAOs. (However, the NOSTAR deletion (31) is actually fully variational, so that large self-consistency errors are also prevented in this limit.)

In the actual program implementation, the NBO segments must access the energy evaluation and geometry optimization routines of the host SCF program. Hence, the available deletions options may depend on details of integration with the host SCF program. The interactions to be deleted are specified by a \$DEL keylist, based on the standard orbital labelings of the NBO output or generic relationships between orbitals (all vicinal donor–acceptor interactions, all interactions between distinct molecular units, NOSTAR, etc.).

The \$DEL options provide a powerful, flexible methodology for isolating and characterizing the energetic and structural consequences of specific NAO, NHO, or NBO interactions. Illustrative examples include investigations of internal rotation barriers,³⁹ anomeric effects,⁴⁰ and hydrogen bonding.⁴¹

5.2 Dipole Moment Analysis

NBO/NLMO analysis of the *dipole moment* (invoked by the DIPOLE keyword) provides a rigorous *ab initio* parallel to empirical ‘bond dipole’ schemes.⁴² It also exemplifies principles that can be used to dissect other molecular properties into localized bonding components.

As a starting point, we consider the uncorrelated HF dipole moment $\langle \mu \rangle_{\text{HF}}$ for the 1-electron operator $\hat{\mu}_1$, which can be rigorously expressed as

$$\langle \mu \rangle_{\text{HF}} = \text{Tr}(\hat{\mu}_1 \hat{T}) = \sum_k^{\text{NLMOs}} 2 \langle \tilde{\phi}_k | \hat{\mu}_1 | \tilde{\phi}_k \rangle \quad (32)$$

in terms of doubly occupied NLMOs $\{\tilde{\phi}_k\}$. Each term in equation (32) can be labeled with the Lewis-type NBO that serves

as 'parent' of NLMO $\tilde{\phi}_k$. When NBO \rightarrow NLMO expansions of the form of equation (21) are employed, each NLMO dipole $(\tilde{\phi}_k|\hat{\mu}_1|\tilde{\phi}_k)$ is expressed in terms of its parent Lewis-type NBO and the residual non-Lewis-type NBOs. The dominant NBO dipole moment contribution is localized and highly transferable, whereas the residual non-Lewis contributions (labeled 'deloc' in the program output) reflect the charge shifts due to conjugative donor-acceptor interactions with the surrounding environment that are the principal sources of non-additivity and non-transferability. Note that even slight population shifts between Lewis and non-Lewis orbitals can produce appreciable dipole moment corrections, owing to the rather large separations of orbital centroids that are characteristic of intra- or intermolecular donor-acceptor interactions.

For post-HF levels, the summation in equation (32) includes cross-terms between NLMOs and slight population deviations from 2 that are appended as a 'correlation correction' to the above terms.

It should be emphasized that the localized A-B bond dipole is not simply equal to the product $Q_A Q_B R_{AB}$ of the atomic natural charges and their separation distance. This all-too-common assumption is valid only for isolated point charges (delta-function distributions), and is particularly unrealistic for A-H hydride bonds.⁴³ It is therefore fundamentally incorrect to 'assess' an atomic charge on the basis of whether it supports this fallacious assumption. NPA is inherently consistent with molecular and bond dipole moments, when the latter are properly evaluated as integrals over the dipole moment operator.

5.3 Natural Steric Analysis

NBO analysis of steric interactions (invoked by the STERIC keyword) is based on identifying the interatomic 'exchange repulsion' energy component E_{exch} associated with wavefunction *antisymmetry*.⁴⁴ Following Weisskopf,⁴⁵ the 'kinetic energy pressure' associated with *exchange repulsions* is pictured as arising from the increased nodal structure (and higher wavefunction curvature near nodal oscillations) required to preserve the mutual orthogonality of filled orbitals on atoms that are forced into close spatial proximity. Thus, for a wavefunction which is well described by $N/2$ doubly-occupied NBOs, E_{exch} can be identified with the energetic cost of the interatomic orthogonalization that converts each pre-orthogonal PNBO $\tilde{\sigma}_I$ into the corresponding NBO σ_I . In the Hartree-Fock framework, this energy increase can be directly evaluated in terms of diagonal Fock matrix elements:

$$E_{\text{exch}} = \sum_I^{N/2} \left(F_{I,I}^{(\text{NBO})} - F_{I,I}^{(\text{PNBO})} \right) = \sum_I^{N/2} \left(\langle \sigma_I | \hat{F} | \sigma_I \rangle - \langle \tilde{\sigma}_I | \hat{F} | \tilde{\sigma}_I \rangle \right) \quad (33)$$

evaluated in the NBO or PNBO basis respectively. Note that expression (33) includes intra-bond effects of covalent bond formation as well as inter-bond contributions, but omits the exchange interactions within isolated atoms. Thus, E_{exch} vanishes in the limit of isolated atomic fragments, consistent with retaining only the terms contributing to steric repulsion between atoms.

It is also possible to approximate E_{exch} in terms of the pairwise-additive sum ($E_{\text{exch}}^{(\text{pw})}$) of localized steric exchange

($E_{I,J}^{\text{exch}}$) between distinct Lewis-type NBOs,

$$E_{\text{exch}}^{(\text{pw})} = \sum_{I < J}^{N/2} E_{I,J}^{\text{exch}} \simeq E_{\text{exch}} \quad (34)$$

$E_{\text{exch}}^{(\text{pw})}$ corresponds closely to the physical picture of direct steric contact between localized electron pairs, as usually implemented in empirical models of steric interactions. Each contributing $E_{I,J}^{\text{exch}}$ is evaluated from partially deorthogonalized 'PNBO/2' orbitals which incorporate only an inverse 2×2 occupancy-weighted symmetric orthogonalization between NBOs I, J ,

$$E_{I,J}^{\text{exch}} = \left(F_{I,I}^{(\text{NBO})} - F_{I,I}^{(\text{PNBO}/2)} \right) + \left(F_{J,J}^{(\text{NBO})} - F_{J,J}^{(\text{PNBO}/2)} \right) \quad (35)$$

Although the pairwise-additive approximation of equations (34) and (35) is adequate for many purposes (and in good correspondence with empirical steric concepts), it should be emphasized that exchange repulsions are inherently a collective response of the entire N -electron system, rather than a set of pairwise changes (equation 35) that can be treated as independent and additive.

NBO steric exchange differences:

$$\Delta E_{\text{exch}}(\text{A} \cdots \text{B}) = E_{\text{exch}}(\text{A} \cdots \text{B}) - E_{\text{exch}}(\text{A}) - E_{\text{exch}}(\text{B}) \quad (36)$$

are found to give an excellent description of the repulsive potentials between rare gas atoms. By choosing a fixed probe species B (e.g., He atom) and equating the $\text{A} \cdots \text{B}$ steric repulsion to the ambient thermal kinetic energy of collisions ($kT \simeq 0.6 \text{ kcal mol}^{-1}$ at 300 K), one can also determine a natural 'steric radius' r_A for which

$$\Delta E_{\text{exch}}(\text{A} \cdots \text{B}) = kT \text{ at } R_{\text{A} \cdots \text{B}} = r_A + r_B \quad (37)$$

Natural steric radii determined from equation (37) are generally in good qualitative agreement with the idealized van der Waals spheres assumed in empirical treatments of steric phenomena. However, criterion (37) provides a more detailed picture of the steric surface topography, including non-spherical contours, interstitial regions, and possible dependences on the probe species B. Further details of the steric surface and recommended natural steric radii for many atomic and ionic species are presented in the original work.⁴⁴

5.4 Natural Energy Decomposition Analysis

The natural energy decomposition analysis (the keyword is NEDA) of Glendening and Streitwieser⁴⁶ provides a more comprehensive picture of the various energy components contributing to intermolecular interactions. The NEDA decomposition mimics in some ways the older Kitaura-Morokuma⁴⁷ analysis, but it avoids the use of non-orthogonal (and exclusion principle-violating) wavefunctions for the two monomers, with the attendant interpretational ambiguities.

NEDA results in an expression for the (counterpoise corrected) interaction energy $\Delta E(\text{A} \cdots \text{B})$ of an $\text{A} \cdots \text{B}$ complex as a sum of 'charge transfer' (ΔE_{CT}), 'electrostatic' (ΔE_{ES}), and 'deformation' (ΔE_{DEF}) components,

$$\Delta E(\text{A} \cdots \text{B}) = \Delta E_{\text{CT}} + \Delta E_{\text{ES}} + \Delta E_{\text{DEF}}(\text{A}) + \Delta E_{\text{DEF}}(\text{B}) \quad (38)$$

Each component is closely tied to NBOs of the A...B supermolecule wavefunction ψ_{AB} , evaluated for a chosen separation R .

Starting from the density matrix in the NBO basis, one first calculates the eigenvectors of the A-fragment block to construct the determinantal wavefunction $\psi_A^{(\text{def})}$ for the deformed fragment A in the complex (and similarly $\psi_B^{(\text{def})}$ for the B-fragment). The energy change $\Delta E_{\text{DEF}}(\text{A})$ required to distort the wavefunction for isolated A ($\psi_A^{(\infty)}$) to its final deformed form in the complex ($\psi_A^{(\text{def})}$) can be evaluated as (similarly for B)

$$\Delta E_{\text{DEF}}(\text{A}) = \langle \psi_A^{(\text{def})} | \hat{H}_A | \psi_A^{(\text{def})} \rangle - \langle \psi_A^{(\infty)} | \hat{H}_A | \psi_A^{(\infty)} \rangle \quad (39a)$$

$$\Delta E_{\text{DEF}}(\text{B}) = \langle \psi_B^{(\text{def})} | \hat{H}_B | \psi_B^{(\text{def})} \rangle - \langle \psi_B^{(\infty)} | \hat{H}_B | \psi_B^{(\infty)} \rangle \quad (39b)$$

where

$$\hat{H} = \hat{H}_A + \hat{H}_B + \hat{H}_{AB} \quad (40)$$

is the usual partitioning of the full Hamiltonian into fragment (\hat{H}_A, \hat{H}_B) and coupling (\hat{H}_{AB}) terms. If the fragments are outside van der Waals contact, $\Delta E_{\text{DEF}}(\text{A})$ is principally the energy penalty to polarize the A wavefunction in the electrostatic field due to B, but at smaller separations it includes the steric repulsions penalty to prevent Pauli-violating interpenetration of the A, B charge distributions. Thus, the deformation energies $\Delta E_{\text{DEF}}(\text{A})$, $\Delta E_{\text{DEF}}(\text{B})$ are intrinsically positive, reflecting, e.g., the deviation of $\psi_A^{(\text{def})}$ from its variationally optimal isolated form $\psi_A^{(\infty)}$. Note that the deformation components (39a,b) (as well as other components to be discussed below) are evaluated in the complete basis set of the complex, so that they automatically include the full counterpoise correction⁴⁸ to remove numerical artifacts of basis set superposition error.

For the full A...B complex at separation R , the localized determinantal wavefunction built from the two deformed fragments $\psi_A^{(\text{def})}$, $\psi_B^{(\text{def})}$ is

$$\psi_{AB}^{(\text{loc})} = 2^{-1/2} \det | \psi_A^{(\text{def})} \psi_B^{(\text{def})} | \quad (41)$$

This is employed to evaluate the 'electrostatic' component ΔE_{ES} as

$$\Delta E_{\text{ES}} = \langle \psi_{AB}^{(\text{loc})} | \hat{H} | \psi_{AB}^{(\text{loc})} \rangle - \langle \psi_A^{(\text{def})} | \hat{H}_A | \psi_A^{(\text{def})} \rangle - \langle \psi_B^{(\text{def})} | \hat{H}_B | \psi_B^{(\text{def})} \rangle \quad (42)$$

Note that this differs in two respects from earlier⁴⁷ treatments of electrostatics. First, one usually expresses the electrostatic interaction with respect to two unpolarized wavefunctions ($\psi_A^{(\infty)}$, $\psi_B^{(\infty)}$), whereas equation (42) is expressed in terms of the actual distorted forms of the fragment wavefunctions ($\psi_A^{(\text{def})}$, $\psi_B^{(\text{def})}$) within the complex. The ΔE_{ES} component therefore contains residual polarization contributions [beyond those included in $\Delta E_{\text{DEF}}(\text{A})$, $\Delta E_{\text{DEF}}(\text{B})$] that arise from the interaction of permanent electric moments of one fragment with the induced moments of the other. Second, earlier treatments generally evaluated an integral such as equation (42) using a Hartree-product ($\psi_A^{(\infty)} \psi_B^{(\infty)}$) of fragment wavefunctions, thereby neglecting interfragment exchange effects. The

corresponding NEDA integral (equation 42) employs a fully antisymmetrized wavefunction (equation 41), so that exchange effects are always properly incorporated. Finally, the 'charge transfer' component ΔE_{CT} is evaluated as

$$\Delta E_{\text{CT}} = \langle \psi_{AB} | \hat{H} | \psi_{AB} \rangle - \langle \psi_{AB}^{(\text{loc})} | \hat{H} | \psi_{AB}^{(\text{loc})} \rangle \quad (43)$$

This represents the variational energy lowering (stabilization) as the localized fragments $\psi_{AB}^{(\text{loc})}$ are able to delocalize between fragments to form the final ψ_{AB} . Note that equation (43) effectively includes all possible interactions (donor-donor, donor-acceptor, acceptor-acceptor) between NBOs of the A and B fragments. However, only the donor-acceptor interactions (of the type previously discussed) are found to contribute significantly to the CT component.

To further assist in dissecting electrostatic interactions, NEDA calculates the fragment dipole moments $\mu_A^{(\infty)} = \langle \psi_A^{(\infty)} | \hat{\mu} | \psi_A^{(\infty)} \rangle$ and $\mu_A^{(\text{def})} = \langle \psi_A^{(\text{def})} | \hat{\mu} | \psi_A^{(\text{def})} \rangle$ (and similar $\mu_B^{(\infty)}$, $\mu_B^{(\text{def})}$) in the isolated and deformed fragments. The difference between these two vector quantities is a measure of the induced dipole for a fragment in the complex. Such quantities have been shown to reduce smoothly to the expected classical electrostatic limits as the A...B separation increases beyond van der Waals contact. Thus, the NEDA components appear fully consistent with the expected asymptotic classical multipole behavior in the long-range limit where exchange effects are negligible (roughly, beyond the sum of the r_A , r_B natural steric radii), but they differ appreciably from classical electrostatic estimates at smaller A...B separations where CT and exchange effects grow rapidly.

NEDA has been applied to a variety of molecular complexes,⁴⁹ including ternary and higher clusters. The NEDA results are fully consistent with other NAO/NBO analyses discussed above, but they are advantageous in providing a comprehensive and unified 'single-pass' overview of contributions to intermolecular interaction (including counterpoise-corrected energetics) for any chosen geometry of the complex.

5.5 Natural Chemical Shielding Analysis

Natural chemical shielding analysis⁵⁰ (keyword NCS) provides a localized NBO/NLMO-based description of NMR chemical shielding tensors calculated in the framework of the GIAO (gauge-including atomic orbital) method.⁵¹ NCS analysis thereby serves to relate GIAO chemical shifts to specific structural features of the chemical environment. Similar localized orbital decompositions were originally introduced in the alternative IGLO⁵² and LORG methods⁵³ to achieve improved gauge-invariance and interpretability. NCS analysis allows the interpretive advantages of non-GIAO localized treatments to be combined with the intrinsic numerical efficiency and accuracy of the GIAO approach.

The starting point for NCS analysis is the GIAO expression for the anisotropic NMR chemical shielding tensor components $\sigma_{\alpha\beta}$ as a sum of 'unperturbed' (u) and 'induced' (i) contributions,

$$\sigma_{\alpha\beta} = \text{Tr}\{\mathbf{D}^{00} \mathbf{h}^{\alpha\beta}\} + \text{Tr}\{\mathbf{D}^{a0} \mathbf{h}^{0\beta}\} = \sigma_{\alpha\beta}^{(u)} + \sigma_{\alpha\beta}^{(i)} \quad (44)$$

where the matrices \mathbf{D}^{00} , \mathbf{D}^{a0} , $\mathbf{h}^{0\beta}$, and $\mathbf{h}^{\alpha\beta}$ represent respectively the Fock-Dirac density matrix, the density derivative with respect to magnetic field component B_α , the derivative

of the 1-e Hamiltonian (**h**) with respect to magnetic moment component m_β , and the crossed second derivative of **h** with respect to M_α and m_β , all in the basis of atomic orbitals $\{\chi_p\}$. For the full chemical shielding anisotropy, the tensor indices α, β range over the Cartesian components x, y, z , but the isotropic scalar shielding (average diagonal component):

$$\sigma_{\text{iso}} = \frac{1}{3} \sum_{\alpha=1}^3 \sigma_{\alpha\alpha} \quad (45)$$

is the quantity of principal chemical interest. Note that the respective contributions $\sigma_{\alpha\beta}^{(u)}, \sigma_{\alpha\beta}^{(i)}$ correspond crudely to 'diamagnetic' and 'paramagnetic' contributions in Ramsey's original (non-GIAO) treatment, inasmuch as $\sigma_{\alpha\beta}^{(u)}$ arises solely from the unperturbed field-free wavefunction, whereas $\sigma_{\alpha\beta}^{(i)}$ is the field-induced contribution of excited states.

The formal similarity of the components in equation (44) to other one-electron properties (e.g., equation 32) suggests how one can similarly use NLMO and NBO expansions of the density matrix (or its derivatives) to identify localized contributions to $\sigma_{\alpha\beta}^{(u)}, \sigma_{\alpha\beta}^{(i)}$. The final expressions are of the form

$$\sigma_{\alpha\beta} = \sum_j^L \left[j\sigma_{\alpha\beta} + \sum_n^{\text{NL}} j \rightarrow^n \sigma_{\alpha\beta} \right] \quad (46)$$

where $j\sigma_{\alpha\beta}$ is a Lewis-type (L) contribution from the parent NBO of NLMO $\tilde{\phi}_j$ (with index j serving to identify both the NLMO and its parent NBO), and $j \rightarrow^n \sigma_{\alpha\beta}$ is a non-Lewis-type (NL) contribution from the 'delocalization tail' of this NLMO; cf. equation (17). Each $j \rightarrow^n \sigma_{\alpha\beta}$ is therefore the shielding associated with a particular donor-acceptor interaction (Sections 3.2.2 and 5.1), contributing only when conjugative or hyperconjugative delocalization is present. Note that such delocalization occurs in both ground and excited states, so NL contributions to both $\sigma_{\alpha\beta}^{(u)}$ and $\sigma_{\alpha\beta}^{(i)}$ are possible. The detailed expressions for $j\sigma_{\alpha\beta}, j \rightarrow^n \sigma_{\alpha\beta}$ are beyond the scope of the present article.

Compared with other molecular properties, NMR chemical shieldings are found to be less sensitive to long-range hyperconjugative and conjugative delocalization effects, with far the largest and most transferable contribution coming from the innermost core orbitals of the shielded nucleus. However, the shift with respect to a chosen reference nucleus reflects differential changes of the valence shell shielding (as well as weaker shieldings due to electrons of adjacent atoms) that are of primary chemical interest. Despite the relatively smaller role of hyperconjugative non-Lewis contributions $j \rightarrow^n \sigma_{\alpha\beta}$, such effects are found to be significant in certain cases (e.g., shielding of oxygen nucleus in formaldehyde, due to $n_O \rightarrow \sigma_{\text{CH}}^*$ hyperconjugation). The non-Lewis contributions also serve to strongly distinguish NCS/GIAO results from those of other localized non-GIAO treatments (IGLO, LORG), since in the latter case these terms are implicitly mixed into 'bond' contributions, with significant degradation of transferability.

A strong benefit of NCS analysis (as in other NAO/NBO decompositions) is the effective reduction to a minimal basis description, comparable to that assumed in qualitative MO theory. This allows many qualitative MO concepts to be usefully applied even when (as usual) the actual GIAO calculations are performed at a far higher theoretical level. For example, Cornwell⁵⁴ showed the usefulness of relating inductive

(paramagnetic) contributions $j \rightarrow^n \sigma_{\alpha\beta}^{(i)}$ to overlap integrals of the form

$$j \rightarrow^n \sigma_{\alpha\beta}^{(i)} \propto \langle b_j(\text{rotated}) | b_n^* \rangle \quad (47)$$

where b_j (rotated) is a local bond-like part of occupied MO j that is spatially rotated (according to the angular momentum component selected by a chosen field component) for overlap with b_n^* , an unrotated antibond-like part of virtual MO n . When visualized with the corresponding NBO contour diagrams, such overlap mnemonics are highly effective in rationalizing the paramagnetic shielding contributions.

6 OTHER NAO/NBO 'ENHANCED' BONDING INDICES AND HÜCKEL-LIKE QUANTITIES

Brief mention may be made of earlier bonding indices (often originating from Hückel MO theory) whose usefulness can be enhanced in the modern *ab initio* context by using NAOs or NHOs. These allow a closer connection to be drawn between the qualitative Hückel-type concepts of elementary valence theory and the quantitative results of rigorous quantum chemical methods.

6.1 Coulson, Wiberg, and Related Measures of Covalent 'Bond Order'

The simplest measure of MO bond order is the Coulson charge and bond-order matrix,⁵⁵ which is essentially the Fock-Dirac density matrix for the minimal basis of occupied valence AOs. When the first-order density matrix is expressed in terms of its NAOs (keyword DMNAO), one obtains a generalization of Coulson's charge and bond-order matrix that exhibits many parallels to the expected Hückel-like patterns, but can be evaluated for an arbitrarily high *ab initio* treatment (HF, DFT, or CI)

Wiberg's bond index⁵⁶ is a related measure of MO bond order, obtained from the (sum of) squared off-diagonal density matrix elements between atoms. The corresponding NAO-Wiberg bond index can be obtained for an arbitrary *ab initio* wavefunction or DFT treatment with the BNDIDX keyword (which also leads to the other bond-order measures discussed below). Unlike the Coulson MO bond order, Wiberg's index is intrinsically positive, making no distinction between net bonding or antibonding character of the density matrix elements. However, it often exhibits closer resemblance to the Pauling bond order⁵⁷ (or to the covalent part of the NRT bond order) than does the corresponding Coulson value.

An alternative 'overlap-weighted NAO bond order' can be obtained by weighting each off-diagonal NAO density matrix element by the corresponding PNAO overlap integral. This avoids the arbitrariness of program-dependent orbital phases (causing each element to appear with the 'correct' sign for bonding or antibonding character) and brings in some details of distance dependence that are absent in the elementary Hückel framework.

An improved bond-order measure of this type was developed by Reed and Schleyer,⁵⁸ called the 'NLMO/NPA bond order.' This is calculated from the compositions of the NLMOs, taking account of both the shared occupancies and the PNAO overlap integrals between atoms.

All of these indices exhibit rather conspicuous deviations from expected classical bond-order values, and each should be considered an approximation to the covalent portion of the NRT bond order (Section 4.1.2). The latter is in greatly improved correspondence with classical valence concepts, and should be considered to supercede earlier types of 'natural bond order.'

6.2 Natural Bond-Bond Polarizability

A chemist often wishes to determine how a disturbance of one bond (e.g., vibrational or photochemical excitation) may alter the properties of other bonds. The 'bond-bond polarizability' $\Pi_{rs;tu}$ was originally introduced by Coulson and Longuet-Higgins⁵⁹ to measure how the Hückel bond order P_{rs} between π -bonded atoms r, s is affected by changing the Hückel interaction parameter β_{tu} between atoms t, u (or conversely, how P_{tu} is affected by changes in β_{rs}),

$$\frac{\partial P_{rs}}{\partial \beta_{tu}} = \frac{1}{2} \frac{\partial^2 E}{\partial \beta_{rs} \partial \beta_{tu}} = \frac{\partial P_{tu}}{\partial \beta_{rs}} = \Pi_{rs;tu} \quad (48a)$$

If $\pi_b = \mathcal{N}[p_r + p_s]$ denotes a pi bond between p-orbitals on atoms r, s , and $\pi_{b'} = \mathcal{N}[p_t + p_u]$ is similarly the bond between atoms t, u , the bond-bond polarizability $\Pi_{b,b'}$ can be formally written as

$$\begin{aligned} \Pi_{b,b'} &= \Pi_{rs;tu} \\ &= 2 \sum_j^{\text{occ}} \sum_k^{\text{vir}} \frac{(c_{rj}c_{sk} + c_{rk}c_{sj})(c_{tj}c_{uk} + c_{tk}c_{uj})}{\varepsilon_k - \varepsilon_j} \end{aligned} \quad (48b)$$

Here c_{rj} , c_{rk} denote the respective LCAO coefficients of p_r in an occupied (ϕ_j) or virtual (ϕ_k) pi MO, with respective orbital energies ε_j , ε_k . For open-shell systems, these quantities are computed separately for alpha and beta spin, with the occupancy factor '2' on the right-hand side of equation (48b) replaced by '1' for each occupied spin orbital.

The natural bond-bond polarizability⁶⁰ (keyword NBBP) gives a full *ab initio* generalization of equation (48b), based on replacing each Hückel p_r by the corresponding NHO h_r and recognizing the formal similarity between the Hückel Hamiltonian matrix \underline{h} and the corresponding *ab initio* Fock (or Kohn-Sham) matrix $\underline{F}^{(\text{NHO})}$ in the NHO basis. For the pi-electron system, the valence NHOs are practically identical to pure p-type AOs as envisioned in Hückel theory, whereas the hybridized NHOs of the sigma system can be used similarly to construct sigma bonds $\sigma_b, \sigma_{b'}$ in all-electron fashion. Note that the NHOs automatically have the proper orthogonality properties assumed in Hückel theory, so the identification of β_{rs} with $(\underline{F}^{(\text{NHO})})_{rs} = \langle h_r | \mathcal{F} | h_s \rangle$ presents no formal difficulty.

The NBBP index $\Pi_{b,b'}$ is closely related to (hyper)conjugative interactions between b, b' bond regions ($b \rightarrow b^*, b' \rightarrow b^*$). Thus, the NBBP values reflect characteristic Hückel-like patterns of pi conjugation as well as more subtle patterns of pi-sigma and sigma-sigma hyperconjugation that govern chemical structure and reactivity.

6.3 Other 'Hückel-like' Methods

The formal association of Hückel β_{rs} with *ab initio* $(\underline{F}^{(\text{NHO})})_{rs} = \langle h_r | \mathcal{F} | h_s \rangle$ matrix elements allows a far-reaching connection to be drawn between older semi-empirical concepts

and modern computational technology (HF or DFT). Starting from the exact NHO Fock matrix (keyword FNHO), one can use perturbative partitioning techniques to analyze the MO eigenvectors into dominant valence-shell 'Hückel-like' contributions (i.e., from a model $\underline{F}^{(\text{NHO})}$ with $\beta_{rs} = \beta \Delta_{rs}$ for valence pi NHOs) and the residual 'non-Hückel' corrections from the full calculation. Such a treatment allows a modern *ab initio* calculation to be mapped onto a low-dimensional model problem of Hückel form as closely as possible.

As discussed in Section 3.2.3, the Fock matrix $\underline{F}^{(\text{NHO})}$ in the NBO basis (keyword FNBO) typically has an even more dramatically simplified form. For qualitative or semi-quantitative purposes:

- (i) all matrix elements beyond the formal valence shell (i.e., beyond the dimension of the formal NMB set) can be essentially ignored;
- (ii) all off-diagonal matrix elements $(\underline{F}^{(\text{NHO})})_{i,j^*}$ of the 'starred' non-Lewis block can be essentially ignored;
- (iii) only the local vicinal matrix elements between a Lewis-type NBO (i) and its neighboring Lewis (j) or non-Lewis (j^*) NBOs need be retained;
- (iv) remaining significant NBO matrix elements are highly transferable from one molecule to another (of similar local geometry), and hence can be approximated with values taken from smaller fragment systems.

These simplifications underlie the usefulness of second-order perturbative analysis of NBO donor-acceptor interactions (Section 3.2.3) in which only the diagonal Lewis-type elements of $\underline{F}^{(\text{NBO})}$ are needed to form the unperturbed 'natural Lewis structure' Hamiltonian.

The simplifying features of the NBO Fock matrix suggest how one may synthesize an approximate model $\underline{F}^{(\text{NBO})}$ using transferable NBO matrix elements from smaller systems. Such model Fock matrices can be used to accurately calculate the MO energy levels of highly extended polyenes, using transferable matrix elements taken from butadiene calculations.⁶¹ The model Hamiltonians of this approach are distinctly 'Hückel-like' in the sense that one retains only a few off-diagonal elements, with identical numerical values between similar bond types. (Indeed, the NBO treatment of a C_{2n} polyene π -system is essentially isomorphic to the corresponding Hückel treatment of a C_n system.)

Jordan and co-workers⁶² have used similar synthetic NBO Fock matrices to analyze through-bond (TB) and through-space (TS) effects in electron-transfer and excitation-transfer processes. Other workers have similarly employed the NBO Fock matrix to examine the patterns of TB/TS interactions,⁶³ demonstrating that the molecular 'transfer pathways' are dramatically different from those envisioned in the McConnell superexchange picture.⁶⁴ As remarked in Section 2, such improved analysis of TB/TS interactions was a primary motivation of the earlier LCBO-MO formulation that preceded NBO theory.

7 SUMMARY AND OUTLOOK

This article has primarily emphasized mathematical and algorithmic aspects of NBO-related methods. We close with

some remarks on broader conceptual and pedagogical implications of these methods and their future development.

It is clear that NBO methods tend to rekindle a sense of optimism concerning the essential *simplicity* and *accuracy* of basic valence concepts. In the past, *ab initio* practitioners often drew overly pessimistic conclusions in this regard (cf. Mulliken's remark: 'The more accurate the calculations become, the more the concepts tend to vanish into thin air.'⁶⁵). NBO analysis gives strong quantitative support to such 'freshman chemistry' concepts as the octet rule, Lewis structure representation, hybridization, Bent's rule, resonance theory, and many others. Transferable orbital and bonding motifs are often found to recur with high fidelity in diverse chemical environments, allowing chemical inferences to be drawn for systems far beyond the reach of full *ab initio* treatment. In the late 1990s, we can explicitly recognize how the simple bonding patterns envisioned by the pioneers of valence theory are truly realized in the best modern wavefunctions.

NBO analysis can also lead to significant *refinements* of classical bonding concepts. Indeed, the NBO framework permits valence concepts to be systematically 'corrected' for higher accuracy or extended to a broader range of phenomena. Examples include determination of higher-order non-additive aspects (cooperative or anticooperative) for intermolecular resonance delocalization² and the emerging paradigms of *sdⁿ* hybridization and hypervalent linear three-center/four-electron interactions ($L: M-L' \leftrightarrow L-M: L'$) in transition metal bonding.⁶⁶

It also seems likely that NBO/NRT methods will play an increasing role in algorithms for *determining* wavefunctions efficiently, as well as in making results of such wavefunctions intelligible to non-specialists. Thus, it is expected that NBO/NRT methods will provide both technical and pedagogical tools for further exploitation of the Schrödinger equation as the ultimate oracle of chemical knowledge.

8 RELATED ARTICLES

Atoms in Molecules; Electron Transfer Calculations; Electronic Wavefunctions Analysis; Hyperconjugation; Intermolecular Interactions by Perturbation Theory; Localized MO SCF Methods; Natural Orbitals; NMR Chemical Shift Computation: Ab Initio; Rotational Barriers: Barrier Origins; Valence Bond Curve Crossing Models.

9 REFERENCES

1. A. E. Reed, L. A. Curtiss, and F. Weinhold, *Chem. Rev.*, 1988, **88**, 899-926; F. Weinhold and J. E. Carpenter, in 'The Structure of Small Molecules and Ions', eds. R. Naaman and Z. Vager, Plenum, New York, 1988, pp. 227-236.
2. F. Weinhold, *J. Mol. Struct. (Theochem)*, 1997, **398**, 181.
3. R. S. Mulliken, *J. Chem. Phys.*, 1952, **23**, 1833-1840.
4. P.-O. Löwdin, *Phys. Rev.*, 1955, **97**, 1474-1489.
5. J. E. Lennard-Jones and J. A. Pople, *Proc. R. Soc. London, Ser. A*, 1950, **202**, 166-180.
6. V. Fock, *Z. Phys.*, 1930, **61**, 126-148.
7. C. Edmiston and K. Ruedenberg, *Rev. Mod. Phys.*, 1963, **34**, 457-465.
8. J. M. Foster and S. F. Boys, *Rev. Mod. Phys.*, 1960, **32**, 300-302.
9. J. E. Carpenter and F. Weinhold, *J. Am. Chem. Soc.*, 1988, **110**, 368-372.
10. F. Weinhold and T. K. Brunck, *J. Am. Chem. Soc.*, 1976, **98**, 3745-3749; T. K. Brunck and F. Weinhold, *J. Am. Chem. Soc.*, 1976, **98**, 4392-4393.
11. It may be noted (cf. Ref. 12) that the name 'natural hybrids' was used much earlier by McWeeny for quite different functions (R. McWeeny, *Rev. Mod. Phys.*, 1960, **32**, 335-369). However, McWeeny's 'hybrids' are found to lack the expected angular characteristics for directional bonding (except in the trivial case of linear molecules, where the correct angular behavior is enforced by symmetry) and apparently found no subsequent applications by other workers. Thus, there is little danger of confusing this earlier usage with modern 'natural hybrid' terminology for the hybrid constituents of NBOs.
12. J. P. Foster and F. Weinhold, *J. Am. Chem. Soc.*, 1980, **102**, 7211-7218.
13. F. Weinhold, 'Quantum Chemistry Program Exchange No. 408', Indiana University, Bloomington, IN, 1980.
14. A. B. Rives and F. Weinhold, *Int. J. Quantum Chem. Symp.*, 1980, **14**, 201-209.
15. A. E. Reed and F. Weinhold, *J. Chem. Phys.*, 1983, **78**, 4066-4073; A. E. Reed and F. Weinhold, *QCPE Bull.*, 1985, **5**, 141.
16. A. E. Reed, R. B. Weinstock, and F. Weinhold, *J. Chem. Phys.*, 1985, **83**, 735-746.
17. P.-O. Löwdin, in 'Perturbation Theory and Its Applications in Quantum Mechanics', ed. C. H. Wilcox, Wiley, New York, 1966, pp. 255-294.
18. R. W. F. Bader, *Acc. Chem. Res.*, 1985, **18**, 9-15.
19. K. B. Wiberg and P. R. Rablen, *J. Comput. Chem.*, 1993, **14**, 1504-1518.
20. B. C. Carlson and J. M. Keller, *Phys. Rev.*, 1957, **105**, 102-103.
21. P.-O. Löwdin, *J. Chem. Phys.*, 1950, **18**, 365-375; P.-O. Löwdin, *Adv. Quantum Chem.*, 1970, **5**, 185-199.
22. R. S. Mulliken, *J. Chem. Phys.*, 1935, **3**, 573-585.
23. H. A. Bent, *Chem. Rev.*, 1961, **61**, 275-311; H. A. Bent, *Chem. Rev.*, 1968, **68**, 587-648.
24. C. A. Coulson, 'Valence', 2nd edn., Oxford University Press, New York, 1961, pp. 203-204.
25. J. E. Lennard-Jones, *Trans. Faraday Soc.*, 1929, **25**, 668-686; R. S. Mulliken, *Rev. Mod. Phys.*, 1932, **4**, 1-86.
26. A. E. Reed and F. Weinhold, *J. Chem. Phys.*, 1985, **83**, 1736-1740.
27. R. S. Mulliken, *J. Phys. Chem.*, 1952, **56**, 295-311.
28. F. Weinhold and J. E. Carpenter, *J. Mol. Struct. (Theochem)*, 1988, **165**, 189-202.
29. J. E. Carpenter and F. Weinhold, *J. Mol. Struct. (Theochem)*, 1988, **169**, 41-62.
30. A. J. McKinley, P. N. Ibrahim, V. Balaji, and J. Michl, *J. Am. Chem. Soc.*, 1992, **114**, 10631-10637.
31. L. Pauling and G. W. Wheland, *J. Chem. Phys.*, 1933, **1**, 362-374; G. W. Wheland and L. Pauling, *J. Am. Chem. Soc.*, 1935, **57**, 2086-2097; L. Pauling, 'Nature of the Chemical Bond', 3rd edn., Cornell University Press, Ithaca, NY, 1960; G. W. Wheland, 'The Theory of Resonance and its Applications to Organic Chemistry', Wiley, New York, 1955.
32. K. F. Freed, *Chem. Phys. Lett.*, 1968, **2**, 255-256.
33. E. D. Glendening and F. Weinhold, *J. Comput. Chem.*, in press; E. D. Glendening, J. K. Badenhoop, and F. Weinhold, *J. Comput. Chem.*, in press.
34. See, e.g., L. Pauling and E. B. Wilson, 'Introduction to Quantum Mechanics', McGraw-Hill, New York, 1935, pp. 374-375.
35. A. C. Hurley, 'Electron Correlation in Small Molecules', Academic Press, New York, 1976.
36. W. Kutzelnigg, in 'Localization and Delocalization in Quantum Chemistry', eds. O. Chalvet, R. Daudel, S. Diner, and J. P. Malrieu, Riedel, Boston, MA, 1975, pp. 143-153.

37. A. V. Nemukhin and F. Weinhold, *J. Chem. Phys.*, 1992, **97**, 1095-1108.
38. W. D. Allen and H. F. Schaefer, *J. Chem. Phys.*, 1987, **87**, 7076-7095.
39. A. E. Reed and F. Weinhold, *Isr. J. Chem.*, 1991, **31**, 277-285; D. Guo and L. Goodman, *J. Phys. Chem.*, 1996, **100**, 12540-12545.
40. P. Petillo and L. Lerner, 'The Anomeric Effect and Associated Stereoelectronic Effects (American Chemical Society Symp. Ser. Vol. 539)', ed. G. R. J. Thatcher, American Chemical Society, New York, 1993.
41. A. E. Reed, F. Weinhold, L. A. Curtiss, and D. J. Pochatko, *J. Chem. Phys.*, 1986, **84**, 5687-5705.
42. O. Exner, 'Dipole Moments in Organic Chemistry', George Thieme, Stuttgart, 1975, pp. 27-54.
43. A. E. Reed and F. Weinhold, *J. Chem. Phys.*, 1986, **84**, 2428-2430.
44. J. K. Badenhoop and F. Weinhold, *J. Chem. Phys.*, 1997, **107**, 5406-5422.
45. V. W. Weisskopf, *Science*, 1975, **187**, 605-612.
46. E. D. Glendening and A. Streitwieser, *J. Chem. Phys.*, 1994, **100**, 2900-2909; E. D. Glendening, *J. Am. Chem. Soc.*, 1996, **118**, 2473-2482.
47. K. Kitaura and K. Morokuma, *Int. J. Quantum Chem.*, 1976, **10**, 325-340; K. Morokuma, *Acc. Chem. Res.*, 1977, **10**, 294-300. Exchange-related artifacts of this method are described by M. Gutowski and L. Piela, *Mol. Phys.*, 1988, **64**, 337-355; R. F. Frey and E. R. Davidson, *J. Chem. Phys.*, 1989, **90**, 5555-5562.
48. S. F. Boys and F. Bernardi, *Mol. Phys.*, 1970, **19**, 553-566.
49. E. D. Glendening, D. Feller, and M. A. Thompson, *J. Am. Chem. Soc.*, 1994, **116**, 10657-10669; M. B. More, E. D. Glendening, D. Ray, D. Feller, and P. B. Armentrout, *J. Phys. Chem.*, 1996, **100**, 1605-1614; E. D. Glendening and D. Feller, *J. Phys. Chem.*, 1996, **100**, 4790-4797; E. D. Glendening and D. Feller, *J. Am. Chem. Soc.*, 1996, **118**, 6052-6059.
50. J. A. Bohmann, F. Weinhold, and T. C. Farrar, *J. Chem. Phys.*, 1997, **107**, 1173.
51. F. London, *J. Phys. Radium, Paris*, 1937, **8**, 397-409; H. Hamerka, *Mol. Phys.*, 1958, **1**, 203-215; R. Ditchfield, *Mol. Phys.*, 1974, **27**, 789-807; P. Pulay, J. F. Hinton, and K. Wolinski, in 'Nuclear Magnetic Shieldings and Molecular Structure', ed. J. A. Tossell (NATO ASI Series C, Vol. 386), Kluwer, Boston, MA, 1993, pp. 243-262.
52. W. Kutzelnigg, U. Fleischer, and M. Schindler, in 'NMR Basic Principles and Progress', eds. P. Diehl, E. Fluck, H. Gunther, R. Kosfeld, and J. Seelig, Springer, New York, 1991, Vol. 23, pp. 165-262.
53. A. E. Hansen and T. D. Bouman, in 'Nuclear Magnetic Shieldings and Molecular Structure', ed. J. A. Tossell (NATO ASI Series C, Vol. 386), Kluwer, Boston, MA, 1993, pp. 117-140.
54. C. D. Cornwell, *J. Chem. Phys.*, 1966, **44**, 874-880.
55. C. A. Coulson, *Proc. R. Soc. London, Ser. A*, 1939, **169**, 413-428.
56. K. B. Wiberg, *Tetrahedron*, 1968, **24**, 1083-1096.
57. L. Pauling, L. O. Brockway, and J. Y. Beach, *J. Am. Chem. Soc.*, 1935, **57**, 2705-2709.
58. A. E. Reed and P. v. R. Schleyer, *Inorg. Chem.*, 1988, **27**, 3969-3987; *J. Am. Chem. Soc.*, 1990, **112**, 1434-1445.
59. A. A. Coulson and H. C. Longuet-Higgins, *Proc. R. Soc. London, Ser. A*, 1947, **191**, 39-60; **192**, 16-32.
60. H. E. Zimmerman and F. Weinhold, *J. Am. Chem. Soc.*, 1994, **116**, 1579-1580.
61. J. K. Badenhoop, PhD Thesis, University of Wisconsin Madison WI, 1994, pp. 9-78.
62. K. D. Jordan and M. N. Padden-Row, *Chem. Rev.*, 1992, **92**, 395-410.
63. C. A. Naleway, L. A. Curtiss, and J. R. Miller, *J. Phys. Chem.*, 1991, **95**, 8434-8437; C. Liang and M. D. Newton, *J. Phys. Chem.*, 1992, **96**, 2855-2866.
64. H. M. McConnell, *J. Chem. Phys.*, 1961, **35**, 508-515.
65. R. S. Mulliken, *J. Chem. Phys.*, 1965, **S2**, 43.
66. C. R. Landis, *Adv. Mol. Struct. Res.*, 1996, **2**, 129-161.

Natural Orbital

The orbital defined as the eigenfunction of the spinless one-particle electron density matrix. See *Population Analyses for Semiempirical Methods*.

Natural Orbitals

Ernest R. Davidson

Indiana University, Bloomington, IN, USA

1	Introduction	1811
2	Definitions	1811
3	Utility	1812
4	Summary	1813
5	Related Article	1813
6	References	1813

1 INTRODUCTION

Natural orbitals were defined by P. O. Löwdin¹ as the eigenfunctions of the first-order reduced density matrix. They provide a simple factorization of wave functions for two-electron systems which brings them into a standard, easily interpreted form.^{2,3} For many-electron systems, they provide a basis for constructing Slater determinants so that the importance of the first few terms is maximized. Used in this way, they were the basis for the construction of some of the first accurate wave functions for molecules.⁴ With modern computers, the number of Slater determinants involved in the wave function is no longer so much of an issue and natural orbitals are now mainly used to reduce the wave function and density matrix to a reasonably compact form that facilitates interpretation.

2 DEFINITIONS

A 'one-electron' operator is usually defined as

$$\theta = \sum_{j=1}^N \theta(\mathbf{x}_j) \quad (1)$$

where \mathbf{x}_j stands for the combination of spin, ξ_j , and spatial, \mathbf{r}_j , variables for electron 'j'. The expectation value of this